Atmospheric Environment 293 (2023) 119446

Contents lists available at ScienceDirect

Atmospheric Environment

journal homepage: www.elsevier.com/locate/atmosenv

Review article

# Performance and application of air quality models on ozone simulation in China – A review

Jinya Yang [a], Yu Zhao [a,b,*]

[a] State Key Laboratory of Pollution Control and Resource Reuse and School of Environment, Nanjing University, 163 Xianlin Rd., Nanjing, Jiangsu, 210023, China
[b] Jiangsu Collaborative Innovation Center of Atmospheric Environment and Equipment Technology (CICAEET), Nanjing University of Information Science and Technology, Jiangsu, 210044, China

## HIGHLIGHTS

- GEOS-Chem and CAMx commonly overestimated $O_3$ concentrations in China.
- The correlation coefficient was over 0.5 and NMB was within ±30% in most cases.
- Changed emissions were identified as the major driving force of long-term $O_3$ growth.
- Industry, transportation and biogenic sources contributed almost 80% of $O_3$ in China.
- Current $NO_X$-focused control strategy resulted in a shift to more transitional regime.

## ARTICLE INFO

*Keywords:*
Air quality modeling
Ozone
China
Model evaluation
Emission control

## ABSTRACT

China has experienced increasingly severe $O_3$ pollution in recent years and air quality models (AQMs) have been widely used to understand it and to explore the possible solutions for it. Based on a thorough literature search, this review selected and investigated 212 AQM studies on Chinese $O_3$ since 2010, with different models and spatial scales. We evaluated the model performance of $O_3$ simulation and analyzed the main factors influencing the simulation. The correlation coefficients between simulation and observation were larger than 0.5 and the mean normalized biases (NMB) were within ±30% for nearly 80% of the cases collected from AQM studies. GEOS-Chem and CAMx commonly overestimated the ambient $O_3$ concentration, while the biases for CMAQ, WRF-Chem and NAQPMS were less conclusive. More applications and better model performances were found for the Yangtze River Delta and Pearl River Delta regions. Single-domain simulation provided the best model performance at a horizontal resolution of 12–30 km, and the performance would improve further at 5–10 km with the use of nested-domain and refined local emission inventory. Effective efforts for improvement of the $O_3$ simulation included incorporating chloride reactions with reactive nitrogen species, better considering the interaction with aerosols, and optimizing the parameterization schemes in meteorological processes and the land-use data. AQMs have been mainly applied in interpreting major driving forces and factors influencing $O_3$ level, understanding its source-receptor relationship, and evaluating its environmental impacts and policy effectiveness. Based on the diagnosis and detection of various AQM methods, meteorology seemed to always play a positive and, since the implementation of emission control strategy, increasingly important role on the growth of $O_3$ concentration, and thus should be taken more seriously in the future along with global warming. Source apportionment studies revealed that industry, transport and biogenic sources contributed almost 80% of $O_3$ in China while only around 30% could be attributed to local contribution during $O_3$ episodes in megacities. $NO_X$-focused control measures led to a growth of $O_3$ in urban areas with VOC-limited regime, as well as a shift from VOC-limited to transitional regime in heavily polluted areas of eastern China. VOCs emission control in areas with VOC-limited regime and the negative effect of global warming should be of great concerns on $O_3$ pollution reduction in the future.

* Corresponding author. State Key Laboratory of Pollution Control and Resource Reuse and School of Environment, Nanjing University, 163 Xianlin Rd., Nanjing, Jiangsu, 210023, China.
*E-mail address:* yuzhao@nju.edu.cn (Y. Zhao).

https://doi.org/10.1016/j.atmosenv.2022.119446
Received 16 November 2021; Received in revised form 19 October 2022; Accepted 23 October 2022
Available online 28 October 2022

## 1. Introduction

As a secondary air pollutant and also a climate forcer, ozone ($O_3$) is a key species of the photochemical cycle related deeply to the atmospheric chemical property. It is generated through the complex nonlinear reactions between two main types of precursors, volatile organic compounds (VOCs) and nitrogen oxides ($NO_X$=NO + $NO_2$) (Cohan et al., 2005; FinlaysonPitts and Pitts, 1997). Briefly, in clean air, a photochemical equilibrium exists between NO, $NO_2$ and $O_3$, as shown in reactions (1)–(3), and reaction (3), mentioned as the titration reaction, plays the role of ozone elimination:

$$NO_2 + h\nu(< 420nm) \rightarrow NO_2^* \rightarrow NO + O \quad (1)$$

$$O + O_2 + M \rightarrow O_3 + M \quad (2)$$

$$NO + O_3 \rightarrow NO_2 + O_2 \quad (3)$$

Once biogenic or anthropogenic VOCs are emitted into the atmosphere, their oxidation products including $HO_2$, $RO_2$ and other active intermediate radicals will react with NO:

$$RO_2 + NO \rightarrow NO_2 + RO \quad (4)$$

$$HO_2 + NO \rightarrow NO_2 + OH \quad (5)$$

The above two reactions trigger the conversion of NO to $NO_2$ and act as competitive reactions with the titration reaction. The $NO_2$–NO–$O_3$ system under polluted environment, in the presence of excessive VOCs, constantly consumes NO and supplements the loss of $NO_2$ to promote $O_3$ generation. The process destroys the dynamic balance in the absence of VOCs and causes the gradual accumulation of $O_3$ to uncontrollable concentration (Atkinson, 2000). The formation of $O_3$ in the real atmospheric environment is much more complex, and can be generally classified into three regimes according to its varied nonlinear responses to the precursors. A high ratio of VOCs/$NO_X$ contributes to a $NO_X$-limited regime, and the opposite is VOC-limited. $O_3$ formation is controlled by both VOCs and $NO_X$ under transitional regime. Nevertheless, the reaction paths of VOCs oxidization and other important photochemical radicals involved in the formation of $O_3$, like hydroxyl radical (OH), still remain unclear. All the complexity in the formation mechanism leads to a dilemma for $O_3$ control.

High concentration of troposphere $O_3$ exerts deleterious influences on human health, agricultural production and ecosystem (Avnery et al., 2011; Gryparis et al., 2004; Jerrett et al., 2009; Wittig et al., 2009). In the last decades, China has experienced increasingly severe $O_3$ pollution (Xing et al., 2015). To improve the air quality over the country, the National Air Pollution Prevention and Control Action Plan (NAPPCAP) was issued in 2013, and a series of measures has been conducted on energy conservation and emission abatement (Zhang et al., 2019). However, the summertime daily maximum 8 h average (MDA8) of $O_3$ concentration kept growing at the rate of 1.9 ppb $yr^{-1}$ throughout China during 2013–2019 (Li et al., 2020b). The official observation data from China National Environmental Monitoring Centre (CNEMC) indicated an average of 27 days per year, from 2013 to 2017, with the $O_3$ concentration exceeding the Chinese Grade II Air Quality Standard, defined as MDA8 $O_3$ larger than 160 μg $m^{-3}$ or daily maximum 1 h (DM1) $O_3$ larger than 200 μg $m^{-3}$ (Lu et al., 2018).

Air quality models (AQMs), also known as chemical transport models, are computational numerical 3-D models built to simulate realistic atmospheric chemical conditions. Based on a series of parameterizations and approximations, the observed physical processes, chemical reactions and deposition processes are expressed as multiple mathematical formulas and are integrated into specific models. Driven by the meteorological field and emission inventory input, the mass balance equations for atmospheric species in these models are solved based on the principles of meteorology, atmospheric physics and chemistry and mathematics (Brasseur and Jacob, 2017; El-Harbawi, 2013; Zhang et al., 2011). These processes are conducted in a geographically fixed framework with the modeling domain divided into numerous grid cells, also known as the Eulerian approach. In this way, AQMs estimate the controlling atmospheric processes (e.g., emissions, advection, turbulent diffusion, chemical kinetics, and deposition) to reproduce the formation, transport and fate of atmospheric pollutants, thus estimating the spatial and temporal patterns of concentrations of various atmospheric pollutants (Park and Kim, 2014). AQMs can be classified into two categories as online models and offline models, dependent on whether the model can generate meteorological field by itself. The online (or two-way coupled) models integrate the chemistry into the meteorological model and solve the chemical continuity equations and meteorological equations simultaneously. In contrast, the offline models need to be driven by the meteorological field from weather forecast models and require fewer computing resources. Both types of models are widely used for different research purposes (Brasseur and Jacob, 2017).

AQMs demonstrate unique advantages in air quality studies, including the simulation of pollution pattern at a high spatiotemporal resolution to hour and kilometer level, the interpretation of physical and chemical processes influencing the observed concentration, and the analysis of response of air quality to emission change (Seinfeld and Pandis, 1998; Brasseur and Jacob, 2017; Carmichael et al., 2008). Therefore, AQMs are able to substantially support the scientific research on the mechanisms of air pollution formation and alleviation, and the policy making of cost-effective emission control measures and air quality management. Researchers have applied AQMs to simulate $O_3$ under the planetary boundary layer (PBL) for over two decades in North America, Europe and East Asia (Derwent et al., 2001; Hogrefe et al., 2004; Liu et al., 2005; Sokhi et al., 2006; Wild and Akimoto, 2001).

Given the increasingly severe pollution level, AQMs have been employed by more and more studies to detect $O_3$ pollution and to explore its solution in China. Given the large diversity of research purposes, model selection, and targeted regions, it is difficult to comprehensively understand the capability of $O_3$ simulation and the source and impact of $O_3$ pollution, based on limited individual studies. On the one hand, the model performance indicates the ability to reproduce $O_3$ concentration in the real atmosphere, which is fundamental for further analysis. A summary of model performance could indicate the capabilities of different AQMs to capture the spatiotemporal patterns of $O_3$ by region, and the information is useful for model selection and settings for specific research purposes. On the other hand, the review of model applications could provide the research progress on modeling methods and results for sources and impacts of $O_3$ pollution. Through comparisons between various studies, the common knowledge on $O_3$ pollution could be obtained, and the underlying reasons for any inconsistency could be analyzed. Limitation of current studies, as well as the future research need, can thus be stressed and revealed. In this paper, therefore, we review the model performances on $O_3$ simulation, and model applications in detecting $O_3$ pollution and supporting its control in China. Section 2 gives an overview of the literature investigation. Section 3 looks into the model performance, effects of different factors, and the efforts made for model improvement. Section 4 reviews the applications of $O_3$ simulation for three aspects, including the major influencing factors on $O_3$ level, source-receptor relationship, and the environmental impacts and policy effectiveness. Section 5 summarizes the review.

## 2. Literature investigation

A literature search was conducted using the electronic database Web of Science Core Collection. With “ozone or O3 or O-3”, “chemical transport model or air quality model or CAMx or GEOS-Chem or WRF-Chem or CMAQ”, and “China” as key words, 1520 records matched the query in total published studies from 2000 to 2021. Based on careful examinations of each paper, we found that totally 221 studies conducted air quality modeling to simulate ambient $O_3$ levels within China, and

they were used for analyzing the growth of relevant research activities and constructing the bibliometric network based on the VOSviewer software (van Eck and Waltman, 2010).

As shown in Fig. 1a, the amount of related studies has kept growing for the last two decades particularly since 2013 when the NAPPCAP was issued. Regarding the research issues, Fig. 1b provides the bibliometric analysis of the keywords co-occurrence structure, with the size of the circle indicating the weigh of each keyword and the thickness of the connecting lines representing the linking strength. A clear evolution can be found for the issues related to $O_3$ simulation in China during the last two decades. Before 2010, the studies were more conducated at the continental and intercontinental scales, and China was part of the research focus. During 2010–2016, the research interets were switching to the relationship between individual process (e.g., emissions and chemistry) and $O_3$ concentration. In more recent years, China has experienced servere and complex air pollution, which has driven the research issues to the interaction with aerosols, nonlinear response to precursors and the health impact. The shifting of research interests indicates a gradually deepening understanding on regional $O_3$ pollution in China with AQMs.

Based on the bibliometric analysis, the studies have focused more on the AQM performance of $O_3$ simulation and detection of $O_3$ pollution within China since 2010. We thus selected the publication period of 2010–2021 for further review, and 178 articles were included. In addition, we further searched on the Chinese literature search engine CNKI (China National Knowledge Infrastructure) and added another 34 studies published in Chinese. The number of all the researches added up to 212, and will be presented in the remaining of this review. Fig. 2 provides the numbers of studies by model, spatial scale and region. There were 17 studies conducted at global or continental scale, with China included as a part of the modeling domain. The commonly applied models included the Community Multiscale Air Quality model (CMAQ) and Goddard Earth Observing System with Chemistry model (GEOS-Chem), and other ones were also used like the Community Atmosphere Model with Chemistry (CAM-Chem) and Model of OZone And Related Tracers (MOZART). Seventy-five studies focused on the national scale, accounting for 35% of the reviewed papers. CMAQ, GEOS-Chem and Weather Research and Forecasting with Chemistry model (WRF-Chem), were the mostly applied models, while the Nested Air Quality Prediction Model System (NAQPMS) and other models were also used. Due to its relatively coarse horizontal resolution (mainly 0.5°–2°), in particular, the global model GEOS-Chem was mainly applied at global, continental and national scales. Eighty-seven studies (41%) were conducted at the regional scale, and CMAQ, WRF-Chem and the Comprehensive Air Quality Model with extensions (CAMx) were mainly used. Most of them stressed the three developed urban agglomerations North China Plain (NCP), Yangtze River Delta (YRD), and Pearl River Delta (PRD), and a few focused on SiChuan Basin (SCB) and GuanZhong Plain (GZP) with recent growth of severe $O_3$ pollution. Limited by the reliabilities of local emission inventory and air quality modeling at relatively high resolutions, there are 34 city-scale studies (16%) mainly with CMAQ, WRF-Chem and CAMx. Most of them were conducted for developed megacities or provincial capital cities, such as Beijing, Shanghai, Wuhan and Nanjing.

## 3. The model performance, influencing factors and efforts for model improvement

To examine the overall AQM performance on $O_3$ simulation, we summarize the correlation coefficients (R) and mean normalized biases (NMB) from different studies by model type and region (Fig. 3). Three metrics are included (hourly, MDA8 and DM1 $O_3$ concentration). The median values of R and NMB were 0.73 and 3.6%, respectively, and great diversities existed among studies for both statistics. The R values in 92% and 46% of cases were respectively larger than the "recommended criterion" of 0.5 and the "goal" of 0.75 suggested by Emery et al. (2017). The NMBs in 50% of studies were within the "recommended criterion" of ±15% (Emery et al., 2017), and 78% were within ±30%. However, the ability of models to capture DM1 $O_3$ was poorer, with the mean of NMB and R of −4.6% and 0.64. The results indicate that AQMs were able to approximately reproduce the ambient level of $O_3$ (with a slight overestimation in all and a slight underestimation of peak $O_3$) and to capture its basic spatiotemporal variations (Huang et al., 2021). The positive bias between simulation and observation is consistent with the model evaluations across the world, e.g., North America and Europe. The median of R (0.73) is closed to the average of four review studies over the world at 0.72 (Colette et al., 2011; Emery et al., 2017; Sharma et al., 2017; Solazzo et al., 2017).

CMAQ and WRF-Chem were the mostly used models for $O_3$ simulation in China and the model performances of multiple AQMs are shown

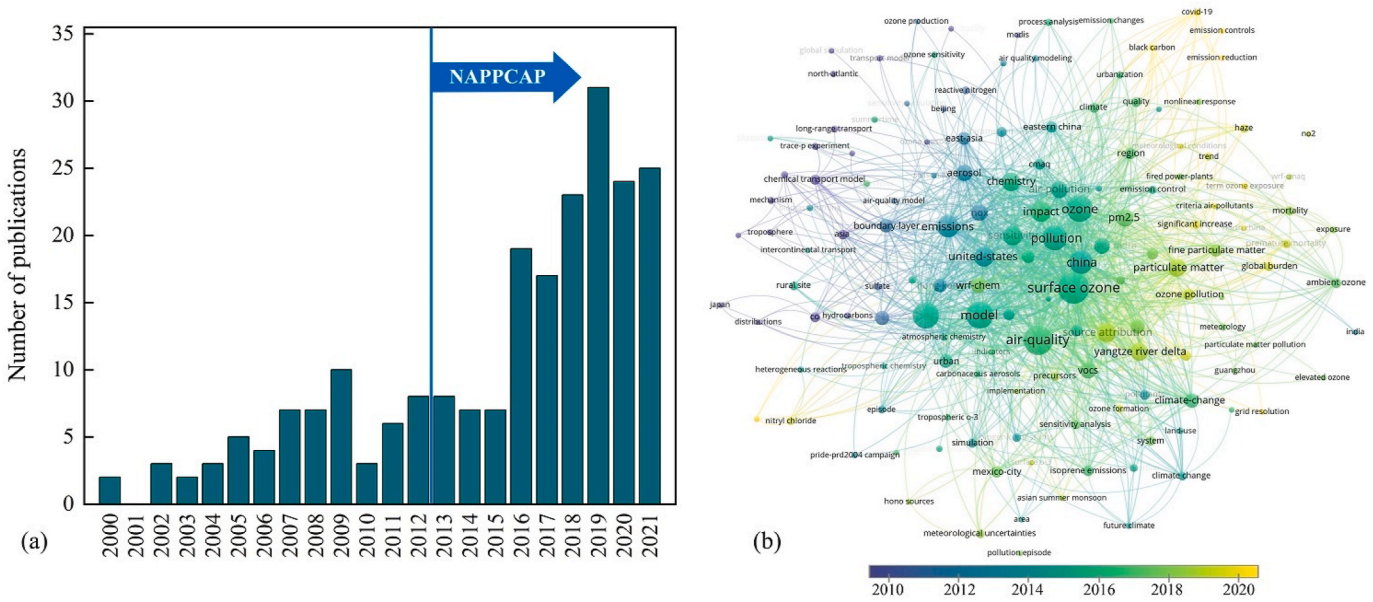


**Fig. 1.** The numbers of Chinese $O_3$ simulation publications by year (a) and the keywords co-occurrence network featured by evolution over time for those studies (b). The size of the circle indicates the weigh of each keyword and the thickness of the connecting line represents the linking strength.

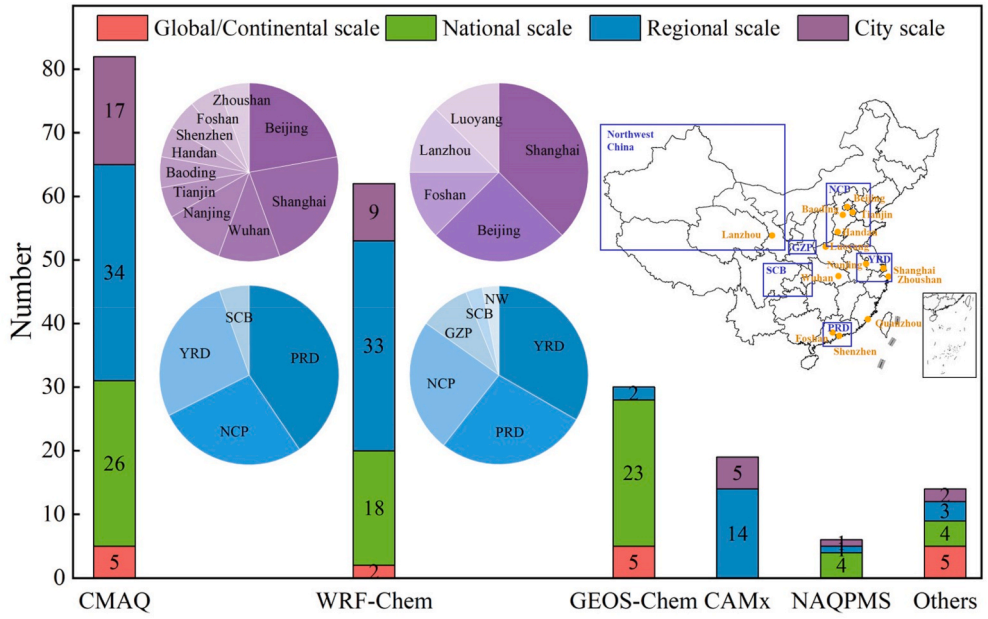


**Fig. 2.** The numbers of Chinese $O_3$ simulation studies by model, spatial scale and region. "Others" refers to the Model for Ozone and Related chemical Tracers (MOZART) and the Community Atmosphere Model with Chemistry (CAM-Chem). NW, NCP, GZP, YRD, SCB and PRD refer to Northwest China, North China Plain, GuanZhong Plain, Yangtze River Delta, SiChuan Basin and Pearl River Delta, respectively.

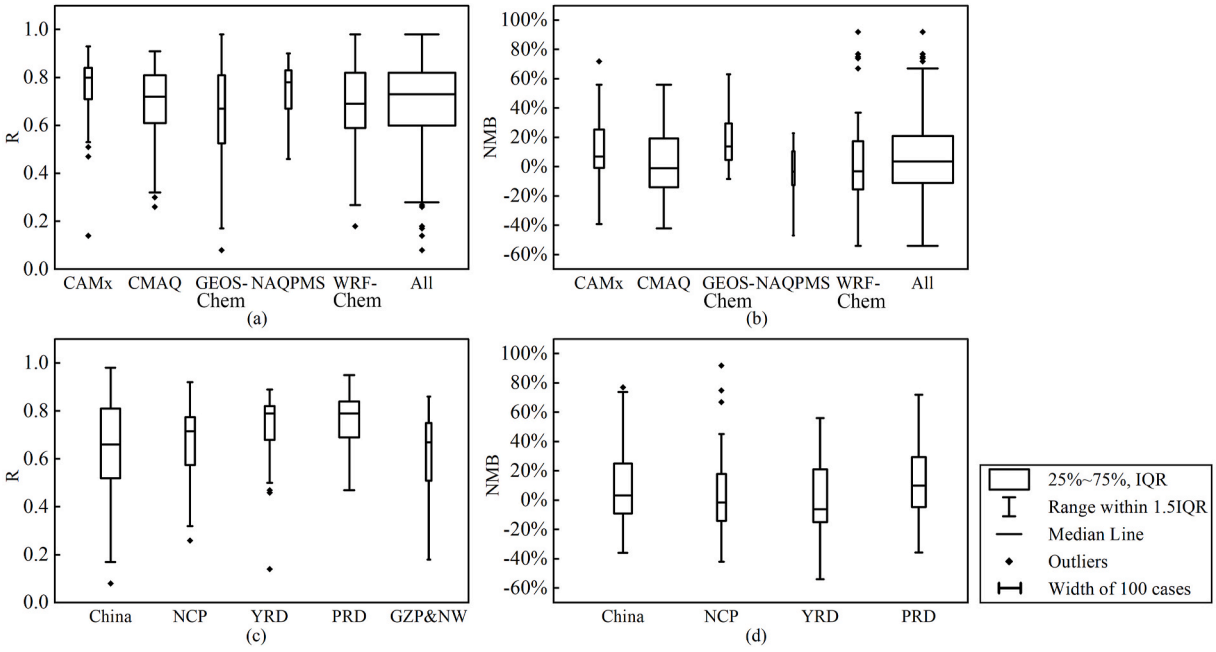


**Fig. 3.** The quantile distributions of correlation coefficients (R) and mean normalized biases (NMB) between the simulated and observed $O_3$ concentrations by model (a and b) and region (c and d). The metrics of hourly, MDA8 and DM1 $O_3$ are not distinguished. Cases grouped into "China" include those focused on eastern China. IQR refers to the Interquartile range, and the width of the boxes indicates the data size.

in Fig. 3a and b. The medians of R ranged between 0.67 and 0.80, with the lowest for GEOS-Chem and highest for CAMx (Fig. 3a). Out of all the models, the biggest interquartile range (IQR) of R (0.28) was found for GEOS-Chem, implying a diverse performance of the model applications. Relatively small IQRs of R were found for CAMx and NAQPMS at 0.12 and 0.16, respectively. Such model performances, however, need further confirmation as the application cases of the two models were much less than CMAQ or WRF-Chem. As shown in Fig. 3b, GEOS-Chem and CAMx commonly overestimated surface $O_3$ concentration in China, indicated by the positive medians of NMBs at 14% and 7%, respectively. No significant bias of overestimation or underestimation was found for CMAQ and WRF-Chem. Positive and negative NMBs were more evenly distributed and the medians of the two models were close to 0.

The medians of R ranged 0.66–0.79 for different regions in China (Fig. 3c). Larger and more consistent R values were found for YRD and PRD. The IQRs of R for the two regions were 0.14 and 0.15, respectively, and the medians of R were 0.79. More diverse model performances existed for NCP and GZP & NW with larger IQRs. No significant difference in NMB appeared between regions, with the medians within ±10% for all regions (Fig. 3d).

Many factors (emission input, horizontal resolution and model mechanisms) influence the model performance of $O_3$ simulation, and they are discussed below. The efforts for the model improvement are correspondingly reviewed as well.

### 3.1. Emission inventory

Emission inventory is the fundamental input of AQMs. The uncertainty of emission inventory, resulting from data availability and/or development methodology, could be passed on to the $O_3$ simulation (Ma and van Aardenne, 2004).

At the national scale, Zhong et al. (2016) conducted WRF-Chem simulations based on the Regional Emission inventory in ASia version 2 (REAS) and the Emissions Database for Global Atmospheric Research version 4.2 (EDGAR). They found comparable $O_3$ simulation performances with the two inventories for July 2007, indicated by the R around 0.8 and NMB around 19% between the simulation and observation. However, a moderate difference of 12–16 ppb was found in some areas including NCP and YRD. Saikawa et al. (2017) used WRF-Chem to assess the difference in $O_3$ simulation for January and July 2008 with REAS v2.1, EDGAR v4.2 and the widely-used Multi-resolution Emission Inventory for China (MEIC). For January, a slight difference was found between REAS and EDGAR simulations, while the $O_3$ levels simulated with MEIC were 31% and 25% lower than those with EDGAR for central and eastern China, respectively. The relatively small VOCs but large $NO_X$ emissions in MEIC were expected to result in a larger titration effect and a more VOC-limited regime. For July, a maximum difference of 8.5 ppb was simulated between the three inventories, and application of REAS resulted in a larger high-$O_3$-polluted area due to the high VOCs emissions. With more observation data in 2013, Hu et al. (2017) compared the WRF-CMAQ performance in $O_3$ simulation, using REAS v2, EDGAR v4.2, MEIC and another inventory from School of Environment in Tsinghua University (SOE). All the simulations met the performance criteria of mean normalized bias within ±15% suggested by USEPA (2001). Slight underestimations (less than 2 ppb) in the annual average $O_3$ concentration were found for the former three inventories, while application of SOE yielded a bigger underestimation at 7.2 ppb. Larger differences between inventories were found in specific regions, like NCP, YRD and SCB. For example, SOE resulted in 5–10 ppb lower DM1 $O_3$ than MEIC in SCB, while REAS predicted up to 10 ppb higher than MEIC in some areas of NCP. Therefore, application of different national inventories could yield more diverse simulations on regional $O_3$ levels than those for the whole country.

With more local emission information at finer horizontal resolution, the model performance at the regional scale would be improved compared to that with the downscaled national emission inventories (Gan et al., 2016). For example, Zhang et al. (2018) updated the emissions from coal-fired power plants in Jiangsu Province in YRD based on the continuous online emission monitoring data. They achieved a better model performance with WRF-Chem and corrected the underestimation of $O_3$ simulation, resulting from the higher VOCs and CO emissions and lower $NO_X$ emissions for the VOC-limited region. Other studies analyzed the uncertainty in $O_3$ simulation, attributed to application of the downscaled national inventory at regional scale. Zheng et al. (2017) found that application of the downscaled national inventory resulted in 12–30% lower $O_3$ in the densely-populated areas but 16–35% higher in the less dense regions for Hebei Province, compared to the simulation with a local inventory incorporating more detailed information of emission sources. The NMBs for the two simulations were −17% and −9%, respectively, indicating a better model performance with local inventory. The difference could be attributed to the weakened associations between the actual emissions and the "spatial proxies" applied for downscaling the national inventory. For example, more polluted industries were moved to suburban or less developed areas, due to the need of air quality improvement for urban regions, while application of the proxies (e.g., population and traffic flow) would allocate more $NO_X$ emissions to the urban region. Given this bias, Zheng et al. (2021) expanded the point source database for China and developed a 1-km resolution emission inventory. Better WRF-CMAQ performance of $O_3$ simulation was obtained than that with MEIC. The spatial correlation between the simulated and observed $O_3$ concentrations was elevated from 0.26 to 0.32 for the country for 2013.

### 3.2. Nested domains and resolution

The domain setting and horizontal resolution in AQMs would influence the meteorology prediction, emission allocation and pollution transport simulation, and thereby the simulation of $O_3$ concentrations (Jiang and Yoo, 2018).

Zheng et al. (2017) investigated the resolution dependence of WRF-CMAQ simulation for Hebei with a local emission inventory. They found that the NMB between $O_3$ simulation and observation for 2013 decreased from 21% to −3% and −9%, when the horizontal resolution was changed from 36 to 12 and 4 km respectively. Tao et al. (2020) applied the NASA UNified WRF (UN-WRF) for NCP 2010, and found that the normalized standard deviation (NSD) decreased from 2.0 to 1.2 when improving the modeling horizontal resolution from 45 to 15 km. With the resolution further improved from 15 to 5 km, little change was found for NSD between simulation and observation. The fine-resolution modeling was especially beneficial to capture high concentration of $O_3$, indicated by the improved capability of reproducing the days exceeding air quality standard. However, limited impact of modeling resolution was found for YRD with WRF-CMAQ simulations at the resolutions of 36, 12 and 4 km, as an emission inventory with relatively coarse resolution of 25 km was uniformly applied for all the simulations (Wang et al., 2021c). Based on a city-scale inventory, Liu et al. (2020) conducted a series of simulations for Nanjing, a typical developed city in YRD, at the resolutions of 36, 12, 4 and 1 km. The NMBs were within ±15% and NMEs were smaller than 25% (the criteria recommended by Emery et al. (2017)) for all the simulations except at the resolution of 36 km, and the best performance was achieved at 12 km.

To further explore the relation between domain setting and model performance, Fig. 4 summarizes 82 studies that provided the R values between simulation and observation out of all the investigated publications. We excluded the global model studies conducted usually at a resolution coarser than 50 km. For single-domain simulations, the best performances were obtained with the horizontal resolutions between 12 and 30 km. When the modeling grid was excessively large, the heterogeneous air quality might not be well reproduced within the grid, and a weak correlation with the observations could be expected. At the resolution under 10 km, application of the downscaled emission inventory with coarse original resolution could bring large uncertainty to the simulation, as discussed in Section 3.1 (Zheng et al., 2017). The

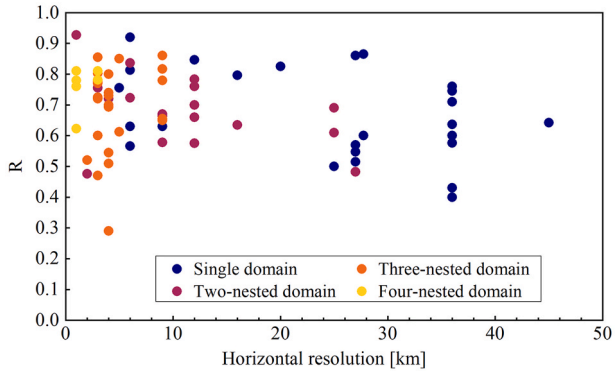


**Fig. 4.** The correlation coefficients (R) between the simulated and observed $O_3$ concentrations in different studies by horizontal resolution of AQM. The finest resolutions were selected for the nested domain studies.

coefficients were commonly larger with finer horizontal resolution for nested-domain simulations, and the simulations with R larger than 0.7 can only be found for the resolutions below 12 km. However, the model performances of different studies varied greatly at a high resolution of 1–5 km. One possible reason could be that current available emission inventories were not all sufficiently precise to support the extremely high-resolution simulation. Overall, the three or even four nested domain setting with the boundary and initial field provided by the mother domain could improve the model performance when the horizontal resolution was below 10 km at the regional or city scale. Along with the increased grid size, the advantages of nested-domain became smaller, and the single domain setting should be appropriate for the simulation at coarser horizontal resolution.

### 3.3. Physical/chemical processes

The model performances for $O_3$ simulation could also be influenced by the diverse applications of physical and chemical mechanisms in AQMs. The model inter-comparison studies evaluated the varied capabilities of $O_3$ simulation over China. Shen et al. (2011) compared the performances of CMAQ and CAMx in PRD for October 2004, and similar spatial patterns of $O_3$ were simulated with a strong correlation with the observations for both. The NMBs of CAMx and CMAQ were 8.8% and −8.5% respectively, due to the higher boundary concentration in CAMx and low $O_3$ photolysis rate in CMAQ. In the Model Inter-Comparison Study for Asia Phase III (MICS-Asia III), Li et al. (2019a) evaluated the performances of 14 state-of-the-art AQMs in $O_3$ concentration simulation over East Asia and reported a considerable inter-model variability by factors of 2–3. Most models were able to capture the diurnal and monthly pattern in NCP, but failed in PRD. Significant overestimations over NCP and PRD were noticed and attributed to the deviation in modeled $O_3$ photochemical production.

The uncertainty of simulation may come from multiple reasons including the model inputs or the model mechanisms. For simulations using GEOS-Chem, the coarse resolution, often at around 0.5°, could lead to an artificial mixed condition of precursors. It might bring areas under different regimes of $O_3$ formation sensitivity into one grid and thus overestimate the concentration under the transitional regime (Yu et al., 2016). Besides, the stronger stratosphere-troposphere exchange (STE), more rapid chemical conversion and less precipitation and cloud cover than the actual were also reported to be the reason for overestimation (Dang et al., 2021; Ni et al., 2018; Sun et al., 2019). For the regional models CAMx and CMAQ, the overestimated $O_3$ was found to often accompany with the underestimated $NO_2$, indicating the insufficient consideration of the titration effect in urban areas in the model (Li et al., 2012, 2013a; Xing et al., 2017). Failure to predict the low concentrations in night-time and winter in CMAQ was reported by Liu et al. (2019a), Hu et al. (2016) and Shu et al. (2016). In contrast, an extremely low level of nighttime $O_3$ was simulated with WRF-Chem (Wei et al., 2018), resulting from the difficulty in resolving the vertical profiles of $O_3$ and $NO_X$ at night. In addition, the uncertainties in the gas-phase chemical mechanism, meteorological conditions, and outdated land-use data were also considered to be responsible for the deviation of CMAQ and WRF-Chem (Liu et al., 2018b; Shu et al., 2016; Zhang et al., 2018). The biases in the simulated $O_3$ concentration, resulting partly from the above-mentioned model limitations, motivated researchers to further improve the model performance in China. The efforts included updating gas-phase mechanism, incorporating chloride reactions with reactive nitrogen species, better considering the interaction with aerosols, and optimizing the parameterization schemes in meteorological processes and the land-use data.

Firstly, gas-phase mechanism used in the model describes the tropospheric chemistry of gaseous species, and it is influential on $O_3$ simulation (Emmerson and Evans, 2009; Jimenez et al., 2003; Zhang et al., 2012). Zhang et al. (2021a) modified the Statewide Air Pollution Research Centre mechanism (SAPRC-11) gas-phase mechanism with updated reaction products of OH with ARO1 (aromatics with $k_{OH} < 1.36 \times 10^{-11}$ $cm^3$ $molec^{-1}$ $s^{-1}$), resulting in a decrease of over 0.5 ppb along the east coast of YRD and NCP. Zhang et al. (2017) incorporated comprehensive chemistry of HONO and nitryl chloride in the Carbon Bond Mechanism (CBMZ_ReNOM) mechanism in WRF-Chem, and the daytime surface $O_3$ concentration was elevated by 4.5 ppb, with the NMB reduced from −12.2% to 0.4% across the country.

Secondly, heterogeneous and gaseous reactions of chlorine species and nitrogen compounds could affect surface $O_3$ concentration by releasing Cl and $NO_2$ or destroying $O_3$ in the photochemical cycles (Simpson et al., 2015; Wang et al., 2019f). These reactions have not been fully incorporated in previous AQM gas-phase and aerosol mechanisms. Li et al. (2016c) developed a chemistry option in WRF-Chem with the heterogeneous uptake of $N_2O_5$ and Cl activation, and investigated their influence on $O_3$ in the Hong Kong-PRD region. This improvement elevated the PBL $O_3$ level by 7.2 ppb (~16.3%) with the NMB of DM1 $O_3$ reduced from −33.2% to −24.8%. With updated gaseous, heterogeneous and aqueous chemistry of chlorine and nitrogen pentoxide in WRF-Chem, the NMB of $O_3$ simulation was slightly reduced from 25.3% to 23.9% in eastern China (Zhang et al., 2021b). Moreover, based on the local anthropogenic chloride emission inventory by Fu et al. (2018), the heterogeneous reactions of nitrogen oxides and chlorides incorporated in CMAQ were estimated to elevate the $O_3$ concentration by up to 20% for some regions in NCP (Qiu et al., 2019). Wang et al. (2020b) and Hong et al. (2020) developed the chloride chemistry in GEOS-Chem and CMAQ respectively, and both of the studies found significant enhancement of $O_3$ concentration in winter due to higher chlorine emissions and adverse meteorological conditions.

Thirdly, aerosols influence the surface $O_3$ level through several ways, like feedback on meteorology and heterogeneous reactions. Efforts have been conducted to improve the coupling of meteorology with chemistry model and aerosol surface chemistry and thereby to optimize the model performance under the complex air pollution in China. Lou et al. (2014) found that the bias of $O_3$ simulation with GEOS-Chem decreased from 33% to 9% for 2005 over China when considering the aerosol impact on heterogeneous reactions and photolysis rate. With the two-way online coupled WRF-CMAQ considering aerosol direct effect, the simulation reproduced lower DM1 $O_3$ level and reduced the NMB from 56% to 42% in high $PM_{2.5}$ polluted days over China in January (Xing et al., 2017). The inclusion of heterogeneous reactions of gases in CMAQ reduced the bias of simulated MDA8 $O_3$ from 11.4 to 6.8 ppb compared to the observation in summertime during 2013–2017 (Liu and Wang, 2020b).

Fourthly, improvement has been made on the meteorology fields, parameterization schemes, and land-use data. Deng et al. (2018) applied CMAQ to evaluate the impact of meteorological models on $O_3$ simulation in PRD and found a difference of 16% in NMB between the simulations based on global/regional assimilation and prediction system (GRAPES) and the fifth-generation Mesoscale Model (MM5). Zhao et al. (2019) selected different PBL and surface schemes in WRF-Chem and found that the simulated $O_3$ concentrations varied from 43.2 to 50.5 ppb in July 2015 over NCP. Zhang et al. (2016) redistributed the vertical profile of emissions, modified the PBL scheme with wind speed bias correction and complemented a new dust emission scheme of Zender et al. (2003) in WRF-Chem. Based on those modifications, they found the $O_3$ simulation performance was improved with the NMB reduced from −11.0–160.3% to −8.8–128.7% over east Asia. Xing et al. (2016) modified the parameterization in STE in CMAQ and found that the STE process contributed 7.4% of the background surface $O_3$ in east China. Li et al. (2014a) applied the up-to-date land cover data with high resolution in GEOS-Chem and found the reduced $O_3$ concentration up to 6 ppb due to the changed dry deposition over China in July 2007. Tao et al. (2018) incorporated the updated land use and land cover change of 2015 in WRF-CMAQ, resulting in a growth of 0.5–4.3 ppb in daytime $O_3$ concentration for Beijing and a decline up to 3.4 ppb in noon $O_3$ for Tianjin in July. While the improved model performances were demonstrated through the above-mentioned efforts, better understandings of

the $O_3$ formation and elimination processes are needed to further reduce the uncertainty in the model mechanisms.

## 4. Applications of AQMs in detection and policy evaluation of $O_3$ pollution

AQMs have been applied to detect the $O_3$ pollution from many perspectives, including interpreting the driving forces and influential factors on $O_3$ level, understanding the source-receptor relationship, and evaluating the impact and policy effectiveness (Brasseur and Jacob, 2017, Fig. 5). They will be reviewed and discussed separately in the following sections.

### *4.1. Interpreting the major driving forces and influencing factors on $O_3$ level*

AQMs could detect the underlying mechanisms and identify the essential factors of the changed air pollutant levels through sensitivity simulations and other specific methods (Brasseur and Jacob, 2017). They acted as a tool for gaining scientific understanding of the observed $O_3$ concentration variations for recent decades in China.

#### *4.1.1. The roles of changed meteorology and anthropogenic emissions*

The $O_3$ concentration has been increasing in different regions of China since 1990 (Shao et al., 2006; Wang et al., 2017). Anthropogenic emissions and meteorological conditions are the two main drivers for the long-term change in $O_3$, and AQMs were commonly applied to figure out their contributions through sensitivity experiments. The contribution of one driver (emissions or meteorology) was quantified by fixing another (meteorology or emissions) at constant during the research period and then subtracting the simulated $O_3$ concentration from the base simulation under actual conditions. Table 1 summarizes the studies which applied AQMs to separate and quantify the contributions of changed emissions and meteorology to the growth of $O_3$ before and during the NAPPCAP.

From the 1980s till NAPPCAP started in 2013, the anthropogenic emissions of $O_3$ precursors ($NO_X$ and VOCs) kept increasing. Fu and Tai (2015) separated the contributions of anthropogenic emissions, climate, and land cover change to $O_3$ level with GEOS-Chem. The result showed an unsurprisingly dominant role of anthropogenic emissions, which enhanced the summer time $O_3$ by 2–25 ppb in East Asia between 1985 and 2005, while the combined effect of climate and land cover changes led to a change from −2 to 12 ppb between 1980 and 2010. The importance of emissions was also emphasized by Fu and Liao (2014). They reported that the increased emissions enhanced summer time $O_3$ by 10–21 ppb, and meteorological parameters and land cover led to a change of −4 to 6 ppb from the late 1980s to the mid-2000s. Sun et al. (2019) conducted simulations with GEOS-Chem between 2003 and 2015 over central-eastern China, and the anthropogenic influence (4.0 ± 1.9 ppb) in the regional average summertime MDA8 $O_3$ was found to be larger than that of meteorology (3.1 ± 4.9 ppb). Jeong and Park (2013) estimated that the changes in emissions and meteorology jointly led to a growth rate of $O_3$ at 0.45 ppb $yr^{-1}$, while the sole contribution from meteorology was 0.13 ppb $yr^{-1}$ in East Asia from 1985 to 2006. Therefore, meteorology was evaluated to contribute 30% to the overall $O_3$ growth. For almost the same period (1986–2006), Yang et al. (2014) estimated an averaged emission-caused $O_3$ change of 5.3 ppb over China. Besides, they applied the absolute percent departure from the mean (APDM) to indicate the interannual variation of $O_3$, and found that the changed meteorological conditions led to an APDM of 1–10% in summertime $O_3$ concentration over China. Lou et al. (2015) simulated $O_3$ concentration from 2004 to 2012, and found that the APDM of tropospheric $O_3$ resulting from the changed meteorological fields was slightly larger than that resulting from the changed emissions across China. However, a larger influence of emissions than meteorology was found in SCB. From a long-term perspective before substantial reduction of precursor emissions in 2013, therefore, most current studies indicated that the prominent growth of emissions played a more influential role on the increased $O_3$ concentration in China.

Since 2013 when the NAPPCAP started, the emissions and concentrations of precursor $NO_X$ have decreased significantly while $O_3$ has kept growing (Fu et al., 2019). Inconsistent findings on the roles of emissions and meteorology were obtained by different studies, and more studies highlighted the importance of meteorological variation on $O_3$ change. Zhang et al. (2021b) applied CAM-Chem and estimated that the changes in annual average MDA8 $O_3$ due to emissions and meteorology were 1.0 and 8.1 ppb respectively between 2010 and 2017. Based on WRF-CMAQ simulation, Ding et al. (2019) estimated the changes of MDA8 $O_3$ due to variation of emissions and meteorology at 0.4–3.7 and −3.5–8.5 ppb by region, respectively, between 2013 and 2017. Liu and Wang (2020a) found that the annual average changing rates in MDA8 $O_3$ resulting from the meteorological and emission variation ranged between −1.5–1.5

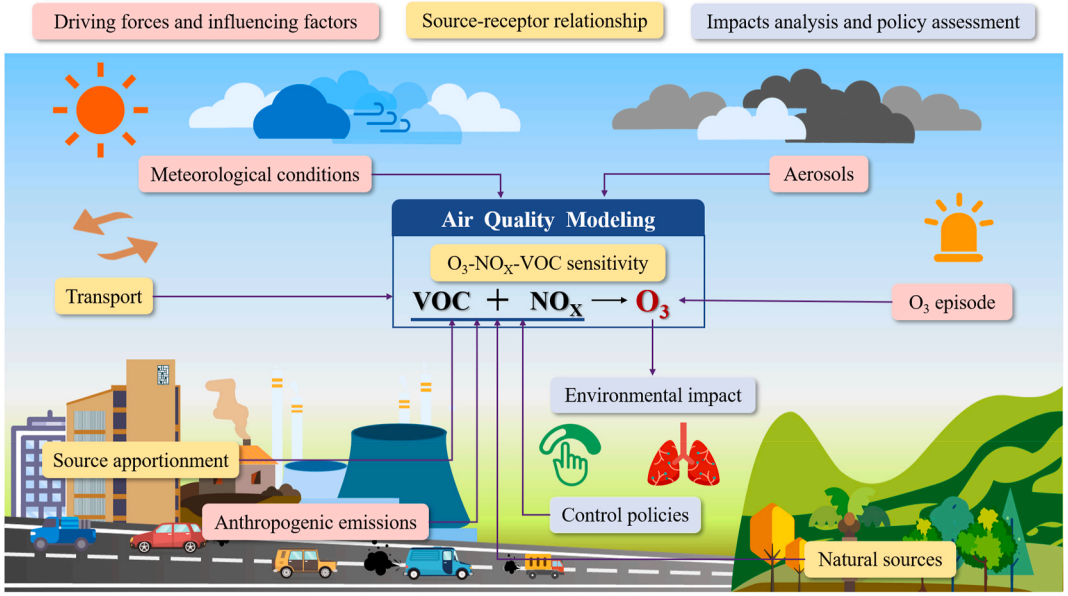


**Fig. 5.** The applications of AQM in detection and policy evaluation of $O_3$ pollution in China.

**Table 1**
Studies on the influence of anthropogenic emissions and meteorological conditions on the changed $O_3$ level in China. The influence is indicated as the changed $O_3$ concentration (ppb), variation rate of $O_3$ concentration (ppb $yr^{-1}$), or APDM (%).

| | Period | Region | Model | Influence of anthropogenic emissions | Influence of meteorological condition | Reference |
|---|---|---|---|---|---|---|
| Before NAPPCAP | 1980 vs. 2010 | East Asia | GEOS-Chem | – | 2–10 ppb | Fu and Tai (2015) |
| | 1985 vs. 2005 | | | 2–25 ppb | – | |
| | 1985–2006 | China | GEOS-Chem | 0.45 ppb $yr^{-1}$[a] | 0.13 ppb $yr^{-1}$ | Jeong and Park (2013) |
| | 1986 vs. 2006 | China | GEOS-Chem | 5.3 ppb | – | Yang et al. (2014) |
| | 1987 vs. 2005 | China | GEOS-Chem | 10–21 ppb | −4 – 6 ppb | Fu and Liao (2014) |
| | 2003 vs. 2015 | Eastern China | GEOS-Chem | 4.0 ± 1.9 ppb[b] | 3.1 ± 4.9 ppb[b] | Sun et al. (2019) |
| | 2004–2012 | China | GEOS-Chem | 1.79% | 1.95% | Lou et al. (2015) |
| | 2010–2017 | China | CAM-Chem | 1 ppb[b] | 5.4 ppb[b] | Zhang et al. (2021b) |
| During NAPPCAP | 2012–2017 | NCP | GEOS-Chem | 0.23 ppb $yr^{-1}$[b] | 0.28 ppb $yr^{-1}$[b] | Dang et al. (2021) |
| | | YRD | | 0.23 ppb $yr^{-1}$[b] | 1.47 ppb $yr^{-1}$[b] | |
| | 2013 vs. 2015 | China | CMAQ | 18.3 ppb[b] | −1.8 ppb[b] | Wang et al. (2019d) |
| | 2013 vs. 2017 | China | WRF-Chem | 0.4–3.7 ppb[b] | −3.5–8.5 ppb[b] | Ding et al. (2019) |
| | 2013 vs. 2017 | Eastern China | WRF-Chem | −9.5–47.0 μg $m^{-3}$[b] | −8.1–21.3 μg $m^{-3}$[b] | Li et al. (2021) |
| | 2013–2017 | China | CMAQ | −1.4–3.2 ppb $yr^{-1}$[b] | −1.5–1.5 ppb $yr^{-1}$[b] | Liu and Wang (2020a) |

[a] Joint influence from both emission and meteorological condition change.
[b] Changes of the MDA8 $O_3$ concentration.

ppb $yr^{-1}$ and −1.4–3.2 ppb $yr^{-1}$ by region during 2013–2017, respectively. Even imposing a smaller interannual change on $O_3$ than emissions, meteorology was identified to be more influential on the spatial pattern of $O_3$, indicated by the consistent variations between the overall change of $O_3$ and that derived from meteorology. A similar conclusion was also made by Dang et al. (2021) that meteorology dominated the spatiotemporal change of $O_3$ concentration over the country from 2012 to 2017. Lu et al. (2019a) analyzed the contributing factors of the increased $O_3$ concentration from 2016 to 2017 with GEOS-Chem. They found that changes in domestic emissions alone would decrease $O_3$ levels, while the hotter and drier weather condition in 2017 offset the anthropogenic efforts. The main reason was that background $O_3$ (in the absence of anthropogenic emissions) accounted for over 80% of total surface $O_3$ at the national scale and it deeply relied on and driven by the meteorology. Wang et al. (2019d) determined the $O_3$ change attributed to meteorological conditions and biogenic emissions by fixing the anthropogenic emissions from 2013 to 2015 in WRF-CMAQ, and the change attributed to anthropogenic emissions was obtained through subtracting the change due to meteorology and biogenic sources from the observed $O_3$ change. They found that the reduced anthropogenic emissions caused 16.7 and 18.3 ppb growth of $O_3$ for provincial capital cities in 2014 and 2015 compared to 2013, respectively, while the contribution of meteorology to MDA8 $O_3$ change was limited (−3.2 and −1.8 ppb). At the regional scale, Dang et al. (2021) detected a similar driving force to MDA8 $O_3$ of emissions in NCP and YRD (0.23 ppb $yr^{-1}$) but a much larger contribution of meteorology in YRD (1.47 ppb $yr^{-1}$) than in NCP (0.28 ppb $yr^{-1}$).

The influence of meteorological changes on $O_3$ could be a joint contribution from multiple factors. For example, temperature influences the natural emissions and the rate of photochemical reaction, while wind fields, boundary layer turbulence and precipitation affect the transport and deposition of $O_3$ (Jacob and Winner, 2009; Li et al., 2017, 2019b; Lu et al., 2019a; Pu et al., 2017; Wang et al., 2017). Studies have been conducted to evaluate the response of $O_3$ to various meteorological conditions in a relatively short term. Ni et al. (2019) applied WRF-Chem to investigate the effect of extratropical cyclogenesis during the 2016 Group of Twenty Finance Ministers and Central Bank Governors (G20) Hangzhou Summit. Abundant passive stratospheric tracers in the low-troposphere along with observed high surface $O_3$ and low CO and humidity confirmed the significant influence of stratosphere intrusion. Li et al. (2016b) investigated the impacts of thermal circulations on $O_3$ formation in PRD with WRF-Chem and found that the urban heat island enhanced turbulent mixing and modified local circulations, leading to a 1.3 ppb decline in daytime $O_3$ and a 5.2 ppb growth around the nighttime rush-hours. Gu and Shu (2010) detected that meteorological condition changes caused by urbanization raised the $O_3$ level by 8.3 μg $m^{-3}$ in urban Shanghai in 2007 with WRF-Chem. Wu et al. (2018) applied WRF-Chem to evaluate the contribution of trans-boundary transport of pollutants dominated by wind fields during the Asian summer monsoon. They indicated that the emissions from the NCP region substantially influenced the northern provinces with a percentage of 15.8–27.4% of the local $O_3$ concentration when the south wind prevailed. Besides, summertime $O_3$ was found to be positively correlated to East Asian summer monsoon index (Yang et al., 2014). With a tagged method in GEOS-Chem, Wang et al. (2011b) identified the monsoonal wind pattern as an important factor in determining background $O_3$ in China. The decreased summertime background $O_3$ could be attributed to the reduced transport of air pollutants from the Europe and North America, which offset the increased transport from Southeast Asia.

To summarize, most studies suggested that China's anthropogenic emissions play a more influential role on long-term $O_3$ growth, while meteorological conditions could also elevate the concentration before the implementation of national air pollution control policies, and might have prevented the $O_3$ concentration declining when the emissions were gradually reduced. The meteorological variation should be emphasized when evaluating the necessity and benefit of emission reduction policies, especially in the context of global warming and climate anomalies (Jacob and Winner, 2009; Lei et al., 2012; Lu et al., 2019b; Sun et al., 2019).

#### 4.1.2. *The influencing factors and processes of $O_3$ pollution episode*

Diagnosis of $O_3$ episode is essential for the early warning of heavy pollution. Based on AQM simulations, the favorable meteorological conditions and the main processes contributing to $O_3$ formation and accumulation could be captured, and the following two main types of studies were conducted:

(1) To obtain the special meteorological conditions of typical $O_3$ pollution episodes compared to non-episode periods, based on the simulated abnormal weather conditions with AQMs.

Gong and Liao (2019) conducted a study on northern China with GEOS-Chem to investigate all the $O_3$ pollution events during 2014–2017. They found a typical weather pattern with high daily maximum temperature, low relative humidity, anomalous southerlies and divergence in the lower troposphere, and some atmospheric dynamic anomaly. Another four studies focused separately on Wuhan (Zeng et al., 2018), SCB (Yang et al., 2020), and YRD (Shu et al., 2016, 2020) draw a similar conclusion that the occurrence of severe $O_3$ pollution was associated with high temperature, strong solar radiation, low wind speed, and low relative humidity. In addition, Hu et al. (2018) reported a regional transport mechanism through nocturnal residual

layer, which resulted in an $O_3$ pollution episode in YRD in 2016. In particular, the location of Wuhan on the periphery of tropical cyclones led to high pressure and subsiding air, and brought surrounding polluted air (Zeng et al., 2018). For PRD, Zeren et al. (2019) indicated that tropical cyclones also played an important role. Weak winds and long residence time for air pollutants, resulting from interactions of synoptic winds and mesoscale breezes, enhanced intensive chemical production of $O_3$.

(2) To evaluate the relative contributions of individual processes to $O_3$ pollution, (e.g., net chemical production, horizontal advection, vertical advection, dry deposition and diffusion), based on the AQMs coupled with integrated process rate (IPR) analysis.

Net chemical production and vertical advection were generally considered as the most dominant processes resulting in $O_3$ episode (Ni et al., 2019). Through GEOS-Chem modeling, the two processes were estimated to cause a change of 3.3 and 8.1 Gg $O_3$ $d^{-1}$ respectively relative to the mean condition for northern China (Gong and Liao, 2019). Yang et al. (2020) applied WRF-CMAQ to simulate the $O_3$ formation in summer of Chengdu, a city in SCB, and found that the vertical transport process accounted for most of the daytime $O_3$ (74.7 ± 5.8%) and horizontal transport process (59.1 ± 9.9%) in nighttime. Shu et al. (2016) conducted WRF-CMAQ simulation for YRD, and estimated that the contribution of vertical diffusion was up to 28.4 and 19.8 ppb $O_3$ $hr^{-1}$ for Shanghai and Hangzhou, respectively, when the $O_3$ concentration was deeply enhanced by the subtropical high and typhoon system. Xu et al. (2018) applied the WRF-Chem to evaluate the contribution of vertical mixing to $O_3$ concentration at different altitudes of an observation station in Nanjing. They found that, during the episode days, photochemical products were generated in the middle and upper PBL and transported to the ground level by vertical mixing, elevating the $O_3$ concentration at a rate of 30 ppb $h^{-1}$. The whole reaction cycle can be explained as following. Abundant $O_3$ production occurred in the upper PBL and resulted in vertical physiochemical circulation in urban areas. $NO_2$, the reaction product of $O_3$ and anthropogenic NO near the surface, was transported vertically to the upper boundary layer where $O_3$ was generated by its photolysis, and then the regenerated $O_3$ would be transported downward to the surface (Tang et al., 2017).

As most current emission inventories could not accurately capture the daily variation in emissions, AQM studies on $O_3$ episodes focused mainly on the meteorology and physical and chemical process. Diagnosed by AQMs, high temperature, low relative humidity and high pressure were typical weather conditions for $O_3$ episodes. Vertical diffusion and net photochemical production accelerated the formation and accumulation of surface $O_3$. More comprehensive causes of $O_3$ episode can be expected with the improved dynamic emission inventories used in AQMs.

#### 4.1.3. The interaction with aerosols

Along with the implementation of NAPPCAP, the $PM_{2.5}$ concentration has dropped sharply across the country while the $O_3$ concentration has kept growing (Chu et al., 2020; Fu et al., 2019). It has been proved that aerosols have a remarkable effect on $O_3$ concentration through multiple pathways, including altering photolysis rates through light scattering and absorption, suppressing the development of PBL, and heterogeneous uptake of gases and peroxide radicals (Gao et al., 2018; Li et al., 2011; Lou et al., 2014; Wai and Tanner, 2010). AQMs, especially those with updated aerosol chemistry mechanisms and online coupled with meteorology models (e.g., online WRF-Chem, two-way coupled WRF-CMAQ, and WRF-GEOS-Chem), were applied to explain the relationship between $O_3$ and aerosols under the complex air pollution in China (Wang et al., 2020a; Xing et al., 2017; Feng et al., 2021).

Using NAQPMS, Li et al. (2011) reported that aerosols changed photolysis frequencies and led to a 5% reduction in PBL $O_3$ in central-eastern China for June 2006. The suppression from aerosols on $O_3$ formation intensified when severe haze episodes occurred. Zhang et al. (2015a) explored the aerosol radiation feedback on air equality in January 2013 with online coupled WRF-Chem. They found that higher aerosol loading resulted in less incoming solar radiation and lower temperature and then reduced ground-level $O_3$ up to 6.9 ppb. Similarly, Wang et al. (2020a) found that the MDA8 $O_3$ was reduced up to 2 ppb by aerosol radiation feedback in most areas of SCB in January 2015. A more significant impact was found in another study for the whole country based on WRF-CMAQ simulation (Xing et al., 2017). Aerosol direct effects, causing changes in atmospheric dynamics and photolysis rates, were estimated to reduce the surface DM1 $O_3$ in January 2013 by up to 39 μg $m^{-3}$. Feng et al. (2016) reported that the ground-level $NO_2$ photolysis frequency was decreased by 30–70% during the daytime and the DM1 $O_3$ was reduced by 20–50 μg $m^{-3}$ from 22 to 24 August 2013 in Xi'an, a city in northwestern China. Gao et al. (2020a) applied the IPR approach and gave a comprehensive explanation on how aerosols influenced the PBL $O_3$ through the changed photolysis rate, for the case of October 2018 over central east China. Ozone production was weakened by the light extinction of aerosol below the PBL, contributing to a larger $O_3$ vertical gradient, and more $O_3$ was then entrained downward from the top of PBL. Therefore, aerosols reduced the $O_3$ not only at the surface but also in the entire PBL. Moreover, black carbon, a typical light-absorbing component of aerosol, could suppress PBL development by heating the air over the PBL, and would then change surface $O_3$ through multiple ways (Ding et al., 2016; Gao et al., 2018). Besides the radiation effect, heterogeneous reactions are also an important factor. With NAQPMS, Li et al. (2018a) reported that heterogeneous reactions reduced more surface $O_3$ concentration (10–20 ppb) than the perturbations from aerosols in photolysis frequencies (1–5 ppb) for the polluted regions of eastern China in 2013.

Since high-level $PM_{2.5}$ suppressed the formation of $O_3$ for the early years of NAPPCAP, whether and how the reduction of $PM_{2.5}$ elevated $O_3$ have been evaluated with sensitivity experiments based on AQMs. Li et al. (2019b) analyzed the driving factors of inter-annual change in summertime surface $O_3$ of eastern China during 2013–2017, by removing the effect of meteorological variability and conducting sensitivity simulations with GEOS-Chem. The result showed that the decreased $PM_{2.5}$ played a more important role on the change of $O_3$ than $NO_X$ or VOCs emission change, as it slowed down the reactive uptake of $HO_2$ radicals that could react with NO and accelerate the $O_3$ accumulation. Liu and Wang (2020b) applied WRF-CMAQ and reported a similar result that the heterogeneous chemical effect rather than the radiative effect contributed most to the increased $O_3$ levels driven by the changed PM concentration. In addition, with more heterogeneous reactions incorporated in CMAQ, they found that the uptake of $O_3$ on aerosol surfaces was also important, following $HO_2$.

However, the $O_3$ and $PM_{2.5}$ concentrations were not always negatively correlated. The rising $O_3$ concentration could raise the primary source of OH (Jacob, 2000) and atmospheric oxidation capacity (AOC), thus in turn enhanced the generation of secondary organic aerosols (SOA). Feng et al. (2019) found consistent growth for the observed $O_3$ and the ratio of organic carbon (OC) to elemental carbon (EC) during the autumns in 2013–2015. They conducted a sensitivity experiment with WRF-Chem to explore the extent to which AOC influenced SOA (represented by OC/EC) during an episode with high concentrations of both $O_3$ and $PM_{2.5}$ in autumn 2015. They found that the SOA level and its fraction in total organic aerosols would decline by 30% and 17% respectively along with 31% reduction in $O_3$ in NCP.

Overall, the complicated relationship revealed by the observed $O_3$ and $PM_{2.5}$ concentrations could be explained by a series of atmospheric physical and chemical processes incorporated in AQMs. Briefly, a high aerosol level suppresses $O_3$ production. When $PM_{2.5}$ concentration goes down, $O_3$ will increase and then enhance AOC and SOA formation (Feng et al., 2016). This interaction calls for further understanding on aerosol chemistry and more thoughts on cooperative control measures of multiple air pollutants (Chu et al., 2020; Zhu et al., 2019).

### 4.2. Understanding the source-receptor relationship of $O_3$

The source-receptor relationship of $O_3$ is complex due to the multiple nonlinear and changing photochemical processes involved in the $O_3$ formation. AQMs were applied to capture the key sources, intermediate species, and dominate processes of $O_3$ formation.

#### 4.2.1. Source apportionment

The complex reactions of $O_3$ formation involve the major precursors, $NO_X$ and VOCs, from both local and regional sources of multiple categories (Atkinson, 2000; FinlaysonPitts and Pitts, 1997; Wild and Akimoto, 2001). Quantification of the contributions of both source categories and regions to surface $O_3$ helps better understand the source-receptor relationship of $O_3$ (Gao et al., 2016; Yang et al., 2019).

At present, there are mainly three types of $O_3$ source apportionment methods based on AQM simulations, i.e., factor separation approach (FSA) based on sensitivity analysis, tagging method, and adjoint model. FSA is usually taken to isolate the effect of one single factor and also its interaction with each other by calculations (Wu et al., 2017). The tagging method is more widely used as it could provide more detailed and convincing information by tracking $O_3$ from different geographic regions and source types through reactive tracer approach (Han et al., 2018). One typical technique is the Ozone Source Apportionment Technology (OSAT) module coupled with CAMx, by which $O_3$ formation is determined into $NO_X$- or VOC-limited at each grid cell and time step and then the contribution is identified by the proportion of specific source to the total regional limiting precursors (Li et al., 2016a; Qiao et al., 2019). Other tagging methods, like the Integrated Source Apportionment Method (ISAM) within CMAQ (Kwok et al., 2015) and 3R approach (Wang et al., 2019c), are similar to OSAT or developed based on it. Adjoint model is a computationally approach to calculate the sensitivity of a scalar model response function with respect to numerous model parameters, such as emissions (Lee et al., 2017; Zhang et al., 2015b).

Utilizing the above methods, source apportionment studies have been conducted at national and regionals scale. Gao et al. (2020b) conducted a series of sensitivity analyses with WRF-Chem to explore the nationwide $O_3$ sources for 2013. They found that $O_3$ formation was more sensitive to industrial and biogenic sources in summer. However, in NCP and YRD, $O_3$ responded negatively to another two important source categories, transportation and power in non-summer seasons due to the VOCs-limited regime. Besides, Li et al. (2017) applied FSA in non-winter seasons of 2015, and identified industry as the most important source in eastern China with the contribution over one fourth to the total $O_3$ concentration in high-polluted days. The second important source was biogenic source in PRD and transportation in other areas.

Given the clear regional difference (Li et al., 2012), a series of studies focused on more targeted and detailed source contributions of $O_3$ formation for specific regions. Fig. 6 summarizes the source apportionment results for four regions with a fast developing economy, i.e., NCP (including specific studies for Beijing and Tianjin), YRD (including specific studies for Shanghai), PRD (including specific studies for Guangzhou and Guangdong Province) and SCB (including specific studies for Chengdu and Chongqing). All the studies applied the tagging method except Gao et al. (2020b) with FSA. As shown in Fig. 6a, the source apportionment results differed for the same region in various studies, attributed to the different methods, research periods, AQM settings, and source categories in the emission inventories. Gao et al. (2020b) (represented by the outer laps for PRD, YRD and NCP in Fig. 6a) yielded a larger contribution from biogenic sources to $O_3$ (about 40–50%) compared to other studies. Another two studies for the PRD region stressed the varied contributions from the same category at different spatial scales. Transportation was estimated to account for 39% of the $O_3$ formation for the developed city Guangzhou (Yang et al., 2019), while the proportion declined to 21% at the provincial level for Guangdong. For Shanghai, Wang et al. (2019c) (the inner YRD lap) reported a contribution of 47% from industry but much less (11%) from transportation, while other studies found more comparable contributions between the two categories. The inconsistency resulted partly from the different considerations of the domains of emissions sources when estimating their contribution to a given area. Wang et al. (2019c) included the sources within an excessively large domain, East Asia, but others selected much smaller regions like YRD or eastern China. Therefore, the contribution of transportation (mainly found in developed urban areas) could be weakened while that of other multiple industrial sources widely located in a broader region could be elevated for the former.

On the whole, the tagging method could reduce the error caused by the non-linearity (Zhu et al., 2017) and provide more reliable and consistent source apportionment results. Fig. 6b provides the averaged source contributions to $O_3$ based on studies with the tagging methods by region. In general, industry, transportation, and biogenic sources were identified as relatively important sources in the four regions, accounting collectively for 80% of the total $O_3$, while power was estimated to contribute around 10%. The result is similar to the national estimation (Gao et al., 2020b; Li et al., 2017). Industry contributed most to $O_3$

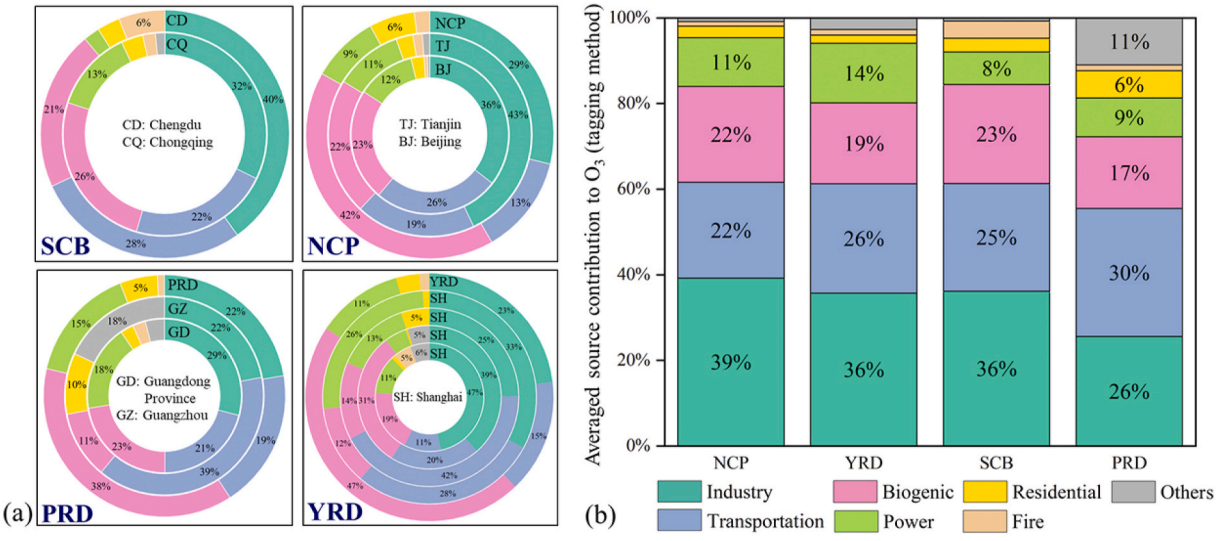


**Fig. 6.** Summary of source apportionment results of ambient $O_3$ for different regions in China (a) and the averaged source contributions to $O_3$ with the tagging method by region (b).

formation with the proportions ranged 36–39% except for PRD, where the contribution from transportation was larger (30%). Biogenic source was another important factor of $O_3$ formation, accounting for around 20% with a slight difference between regions.

The complicated chemical reactions of $O_3$ formation are likely to take a few hours, thus long-range transport could be an important source of $O_3$ (Li et al., 2012; Sharma et al., 2017; Wild and Akimoto, 2001). Li et al. (2014b) evaluated the influence of air pollutants transported from Eurasian areas to $O_3$ concentration in western China in 2000, and the result from sensitivity experiments with MOZART-4 suggested an elevation of 10–15 ppb in 2000. Fu et al. (2012) reported that biomass burning in Southeast Asia could be long-range transported to southern China and even YRD with a contribution of 8–18 ppb in 2006. As a whole, Ni et al. (2018) found that the total foreign anthropogenic emissions contributed 2–11 ppb of $O_3$ over China with several approaches incorporated with GEOS-Chem simulation.

In a regional study based on CAMx-OSAT, the $O_3$ concentration in PRD was found to be more influenced by the sources outside the region for low $O_3$ seasons, while local emissions contributed 50–70% in $O_3$ episodes in autumn and summer 2006 (Li et al., 2013a). Liang et al. (2014) found that under the adverse weather in August 2008, reduction in local emissions without joint control was insufficient for MDA8 $O_3$ in Shenzhen to reach 120 μg $m^{-3}$. With more stringent pollution control measures adopted in megacities, precursors from regional transport played an increasingly important role in recent years. Wang et al. (2021b) conducted adjoint modeling with GEOS-Chem and found that $O_3$ was both sensitive to local and surrounding emissions in the heavily polluted days, while mostly sensitive to local emissions within NCP in other situations. Wu et al. (2017) applied FSA and analyzed that the local and regional emissions independently contributed 22% and 37% to the $O_3$ formation for an $O_3$ pollution episode in July 2015 in Beijing, and that the remaining was attributed to the interaction between the local and regional emissions. Liu et al. (2019a) applied ISAM incorporated in CMAQ and made a similar estimation that the contribution from the boundary condition was up to 77% for the same episode. For another metropolitan Shanghai, Li et al. (2019c) applied OSAT and found that the local emissions contributed 30% to the hourly $O_3$ concentration and that non-Shanghai emissions, mostly from Zhejiang and southern Jiangsu, accounted for the rest in August 2015. Shu et al. (2019) revealed the great importance of super-regional (out of eastern China) transport, with the contributions of 29–51% to several $O_3$ episodes over the whole YRD for 2016, and the contribution was even larger in Shanghai. For Guangzhou, a megacity in PRD, Yang et al. (2019) applied the NAQPMS coupled with an on-line source-tagged module and estimated that the regional transport contributed 73–86% to $O_3$ formation by season in 2015. It can be summarized that regional or super-regional transport accounted for a large proportion of $O_3$ pollution and the local contributions were only around 30% in megacities. The joint prevention and control of regional $O_3$ pollution should be emphasized.

#### 4.2.2. *The contribution of natural sources*

Major natural sources of $O_3$ formation include biogenic VOCs (BVOCs), soil and lightning $NO_X$, and biomass burning emissions (Lu et al., 2019a, 2019b). The natural emissions could be calculated with specific modules like Model of Emission of Gases and Aerosols from Nature (MEGAN, Guenther et al., 2006), and the impact of natural emissions on $O_3$ could be evaluated through sensitivity experiments in AQMs.

From a national perspective, Lu et al. (2019a) found that the BVOCs emissions enhanced more than 15 ppb of MDA8 $O_3$ over central eastern China in summer of 2016–2017. Limited by topographical and geographical factors, influences of other natural sources were mainly found in some particular areas. Lightning and STE, soil emissions, and biomass burning emissions were estimated to collectively contribute over 20 ppb, over 5 ppb, and up to 10 ppb $O_3$ in western China, northern China and Yunnan Province in southwestern China, respectively. Those natural sources were incorporated in GEOS-Chem and some of them were calculated online in the model. With the BVOCs emissions calculated with MEGAN, Wu et al. (2020) reported that the peaked BVOCs emissions in summer greatly enhanced DM1 $O_3$ in eastern and southwestern China up to 47 μg $m^{-3}$. Moreover, influenced by the southerly wind, high BVOCs emissions in southern China were transported to central China and the NCP, and elevated the $O_3$ level in those areas with smaller BVOCs emissions. For the long-term estimation, Fu and Liao (2014) applied GEOS-Chem and found a change of −0.5–0.5 ppb in $O_3$ concentration over China from the late 1980s to the mid-2000s, attributed to the changed land cover and thereby BVOCs emissions. A global study with GEOS-Chem simulation reported that the changed leaf area index and soil $NO_X$ emissions due to nitrogen deposition elevated surface $O_3$ by 2 ppb in north-central China and decreased it by 1 ppb in north China from 1990 to 2010.

Regarding specific regions, Ma et al. (2019) applied WRF-CMAQ and investigated the influences of different factors on BVOCs and then the impact on $O_3$ formation for NCP. They estimated that BVOCs emissions driven by high vapor pressure deficit, land cover change and urban landscape brought an extra 3.1, 2.8 and 4.7 ppb MDA8 $O_3$, respectively. Lu et al. (2021) applied GEOS-Chem and evaluated the roles of soil $NO_X$ on $O_3$ pollution in July 2017. Even though it enhanced the average $O_3$ concentration by only 2.9 ppb, soil $NO_X$ significantly suppressed the sensitivity of $O_3$ to the changed anthropogenic $NO_X$ emissions and thereby weakened the maximum benefit of domestic emission abatement on $O_3$ concentration by 30%. In YRD with abundant forests in the south (Wang et al., 2019e), Liu et al. (2018b) applied WRF-CMAQ and found that the central region was more affected by biogenic emissions with the maximum contribution to hourly $O_3$ at 18–36 μg $m^{-3}$ in July 2014, resulting from the abundant $NO_X$ transported from upwind urban and coastal regions here. They indicated that $O_3$ concentration in rural areas would be more likely to be influenced by BVOCs emissions than urban. Wang et al. (2020c) made a consistent judgment that the contribution of BVOCs to $O_3$ formation was more restricted by $NO_X$ emissions, as similar spatial distributions were found for them. For PRD, Situ et al. (2013) found that BVOCs contributed to a 10-ppb growth of average $O_3$ concentration in summer 2010, with the peak reaching 34 ppb. Besides, heat wave in 2017 was evaluated to elevate the BVOCs contribution to 19.4 μg $m^{-3}$, which was nearly 10 μg $m^{-3}$ higher than the common level (Wang et al., 2021a). For GZP, the most developed region with severe air pollution in northwestern China, abundant BVOCs from the Qinling Mountains interacted with the anthropogenic $NO_X$, yielding 14.4 ppb $O_3$ in urban Xi'an (Li et al., 2018b). Those results all emphasized the combined impact of anthropogenic and natural sources on $O_3$ pollution.

Given the process of global warming and implementation of stricter controls on anthropogenic sources, the natural emissions would be more important on $O_3$ formation, no matter for regions with large local emissions like PRD and YRD or regions strongly influenced by regional transport like NCP. More efforts on interaction between the changed natural and anthropogenic emissions are further needed for better policy making of $O_3$ pollution alleviation.

#### 4.2.3. *$O_3$-$NO_X$-VOCs sensitivity*

As mentioned in the introduction, $O_3$ generation and elimination rely on its nonlinear response to the two types of precursors, briefly summarized as $NO_X$-limited, VOC-limited and transitional regime (Cohan et al., 2005; Jin and Holloway, 2015; Xing et al., 2011a). Three main methods with AQMs have been widely used to determine the photochemical regime of $O_3$ formation in China: photochemical indicators (e.g., $P(H_2O_2)/P(HNO_3)$, $H_2O_2/(O_3+NO_2)$, and $HCHO/NO_2$; Sillman and He, 2002), comparison of the $O_3$ response to the emission change of individual precursor (mentioned as Brute-force method; Sillman and West, 2009), and $O_3$ isopleth. Summarized in Table 2 are the results on $O_3$ formation sensitivity from various studies.

At the national scale, Liu et al. (2010) identified the $O_3$ formation

**Table 2**
Studies on the $O_3$ formation regime at national scale (China) and regional scale (NCP, YRD and PRD). The photochemical indicator with P means the ratio of production rate.

| Period | Target area | Model | Method | Regime (area/time) | Reference |
|---|---|---|---|---|---|
| Jan. 2008 | China | CMAQ | $P(H_2O_2)/P(HNO_3)$ | VOC-limited | Liu et al. (2010) |
| Jul. 2008 | | | | Mainly $NO_X$-limited | |
| Mar. 2010 | China | CALGRID | Brute-force | VOC-limited (urban centers and developed areas)<br>$NO_X$-limited (northern and western areas) | Xie et al. (2014) |
| Aug. 2013 | Eastern China | CMAQ | $(P(H_2O_2)+P(ROOH))/P(HNO_3)$ | Mainly $NO_X$-limited and transitional regime | Wang et al. (2019b) |
| Jul. 2014 | East Asia | WRF-Chem | Brute-force | VOC-limited and transitional regime (urban areas) | Li et al. (2018c) |
| 2016 | Eastern China | CMAQ | Brute-force | VOC-limited and transitional regime (NCP, PRD, YRD)<br>$NO_X$-limited (other areas) | Wang et al. (2019a) |
| 2017 | China | CMAQ | Brute-force | VOC-limited and transitional regime (eastern areas)<br>$NO_X$-limited (western areas) | Shen et al. (2021) |
| Jun. 2008 | NCP | CMAQ | $P(H_2O_2)/P(HNO_3)$ | VOC-limited (urban areas)<br>Transitional regime (suburban and rural areas)<br>$NO_X$-limited (mountainous areas) | Tang et al. (2017) |
| Jul. 2010 | Beijing | WRF-Chem | $H_2O_2/HNO_3$ | VOC-limited (urban areas) | Wei et al. (2018) |
| 2012 | NCP | CMAQ | Brute-force | Mainly VOC-limited | Wang et al. (2019a) |
| Jun. 2015 | NCP | CMAQ | Brute-force | VOC-limited (urban areas)<br>Transitional regime (suburban areas)<br>$NO_X$-limited (remote areas) | Han et al. (2018) |
| Sep. 2009 | Shanghai | WRF-Chem | Brute-force | VOC-limited | Xu et al. (2019) |
| 2012 | YRD | CMAQ | Brute-force | Mainly VOC-limited | Wang et al. (2019a) |
| Jul. 2013 | YRD | CAMx | CAMx-OSAT | Mainly VOC-limited | Li et al. (2016a) |
| Period | Target area | Model | Method | Regime (area/time) | Reference |
| Sep. 2004 | PRD | CMAQ | $O_3$ isopleth | $NO_X$-limited | Wei et al. (2012) |
| Jan. 2004 | PRD | CMAQ | $NO_X/NO_y$ | VOC-limited (central and coastal areas)<br>$NO_X$-limited (rural areas) | Wang et al. (2010) |
| Jan. 2004 | PRD | CMAQ | Brute-force | VOC-limited (central and southern areas)<br>$NO_X$-limited (western, eastern and northern areas) | Wang et al. (2011a) |
| Nov. 2006 | PRD | CAMx | $P(H_2O_2)/P(HNO_3)$ | VOC-limited (morning)<br>$NO_X$-limited (afternoon) | Li et al. (2013b) |
| 2010 | PRD | CMAQ | $P(H_2O_2)/P(HNO_3)$ | VOC-limited (daily averaged)<br>$NO_X$-limited (most areas in the afternoon) | Wang et al. (2016) |
| 2012 | PRD | CMAQ | Brute-force | Mainly VOC-limited | Wang et al. (2019a) |

regime in 2008, using the production rate ratio of $P(H_2O_2)/P(HNO_3)$ with the criterion of 0.2. They estimated that $NO_X$-limited regime dominated almost the whole country in summer except some megacities, and that eastern China was under VOC-limited regime in winter. Xie et al. (2014) applied the Brute-force method and determined the VOC-limited regime for urban centers and $NO_X$-limited regime for northern and western China in March 2010. Shen et al. (2021) found that VOC-limited and transitional regimes covered eastern China while most part of western China was dominated by $NO_X$-limited regime. With rapid decline in $NO_X$ emissions between 2012 and 2016, Wang et al. (2019a) evaluated the changing $O_3$ formation regime by comparing the decreased $O_3$ levels when emissions of the two precursors were reduced separately in WRF-CMAQ. Noticeable changes from VOC-limited to transitional regime were found in the developed NCP, YRD and PRD regions, with the areas of transitional regime increasing from an average of 29%–48% for all the three regions, and other areas in eastern China kept $NO_X$-limited. Similarly, transitional regime was found to cover a wide area over eastern China, while VOC-limited regions were mostly in YRD, PRD and a few other urban centers in August 2013 (Wang et al., 2019b).

More detailed information of $O_3$ formation regime could be found in the AQM studies at the regional scale. For NCP, Han et al. (2018) conducted CMAQ simulation with the Brute-force method and suggested the VOC-limited regime in the urban and other most $O_3$-polluted regions, while the suburban and remote areas were dominated by transitional or $NO_X$-limited regime in summer 2015. The reduced $NO_X$ emissions from power plants were thus not helpful for $O_3$ pollution alleviation in the urban. Besides the difference between urban and rural areas, Tang et al. (2017) found a $NO_X$-limited regime for the mountainous areas of NCP in 2008, based on the indicator of $P(H_2O_2)/P(HNO_3)$ from MM5-CMAQ simulation and the criteria of 0.06 and 0.2 to distinguish VOC-limited, transitional and $NO_X$-limited regimes (Tonnesen and Dennis (2000). Specifically, Beijing was the research hotspot in NCP. According to the ratio of $H_2O_2$ to $HNO_3$ concentration simulated with WRF-Chem and the criteria of 0.35 and 0.65, Wei et al. (2018) implied VOC-limited, $NO_X$-limited and transitional regimes in urban, northern and western rural, and southern and eastern rural areas for July 2010, respectively. Regarding the inter-annual change, Wei et al. (2019) reported that the $O_3$ formation in Beijing changed towards more VOC-limited regime from 2010 to 2013, while it reverted to the 2010 chemistry nature in 2015.

For YRD, Li et al. (2016a) applied the CAMx-OSAT and estimated that VOCs contributed 47–71% to the total $O_3$ in summer 2013. The result suggested that VOC-limited regime occupied most YRD. Based on the WRF-Chem sensitivity experiments, Xu et al. (2019) found a clear VOC-limited regime in urban Shanghai. Both the reduced $NO_X$ and increased VOCs emissions significantly would enhance the $O_3$ concentration from 2009 to 2015.

In PRD, Wei et al. (2012) conducted a series of MM5-CMAQ simulations and obtained the $O_3$ isopleth for September 2004. It was shown that PRD was under $NO_X$-limited regime, and that the VOC-limited regime would occur with the $NO_X$ emissions increasing about 4 times. However, application of one isopleth for the whole PRD region might ignore the spatial heterogeneity in $O_3$ formation regime. Wang et al. (2010) compared the $O_3$ levels between base and emission-reduction cases for October 2004 using MM5-CMAQ, and found that the central and coastal areas of PRD were dominated by VOC-limited regime and the surrounding rural areas in the southwest were $NO_X$-limited. During the same period in central and western PRD, moreover, a temporal shift from VOC-limited regime in the morning to $NO_X$-limited regime in the afternoon was detected by Wang et al. (2011a). Li et al. (2013b) also found a VOC-limited regime in the morning but a $NO_X$-limited regime in the afternoon for November 2006, based on the MM5-CAMx modeled indicator of $P(H_2O_2)/P(HNO_3)$ and a threshold of 035. Wang et al. (2016) applied the same indicator from WRF-CMAQ simulation to

identify the photochemistry in 2010 based on the threshold of 0.4 suggested by Sillman (1995). The regime was generally VOC-limited judged by the daily average ratio, while $NO_X$-limited regime dominated in the afternoon except for some highly-polluted megacities. Scenario analysis suggested that cutting VOCs emissions would decrease overall $O_3$ but cutting the afternoon $NO_X$ emissions would reduce the peak $O_3$ levels.

In general, the AQM studies at different spatial scales suggested a big diversity of $O_3$ formation regime by region and a clear change along with the progress in precursor emission control. VOC-limited and $NO_X$-limited regimes were commonly found in urban centers and rural areas, respectively, and the transitional regime was in surrounding areas of the urban agglomeration. Along with the $NO_X$ control, the VOC-limited region was gradually shifting to the transitional regime in eastern China, and this change could inspire the control strategy adjustment in the future.

### 4.3. Evaluating the environmental impacts and policy effectiveness

AQMs were applied to provide ambient $O_3$ data with large spatio-temporal coverage, which could be further used in environmental impact analysis. They also served as a fundamental tool for policy making, through simulations based on different air pollution control strategies and emission scenarios.

#### 4.3.1. Environmental impact analysis with AQM-derived $O_3$ pattern

Along with the rapid industrialization of China and the continuous global warming, reproducing the long-term historical $O_3$ level helped better understand the impact of human activities on the environment. Based on EDGAR, for example, Xing et al. (2015) obtained the temporal trend in $O_3$ concentration over 1990–2010 with WRF-CMAQ simulation. They found that the MDA8 $O_3$ had been increasing at a rate of 2.57 μg $m^{-3}$ $yr^{-1}$ (1.49% $yr^{-1}$) in eastern China, attributed to the growth in $NO_X$ and VOCs emissions by 4.3% $yr^{-1}$ and 2.3% $yr^{-1}$ respectively.

High $O_3$ concentration is supposed to cause inflammatory response and to be related to some cardiovascular and pulmonary diseases (Gryparis et al., 2004; Xie et al., 2019). The exposure assessment is of great importance for improving public awareness and urging policy making. Based on a national-scale simualtion with NAQPMS, Wang et al. (2020d) estimated the annual averages of respiratory and cardiovascular deaths attributed to $O_3$ exposure at 186,000 (129,000–237,000) and 125,000 (42,000–204,000) during 2013–2017, respectively. Liu et al. (2018a) simulated the $O_3$ concentration and exposure for 2015 at the national scale with WRF-CMAQ. They estimated that a cumulative population of 816 million were exposed to MDA8 $O_3$ over 100 μg $m^{-3}$. The estimated mortality from chronic obstructive pulmonary disease attributed to $O_3$ exposure was in the range of 55,341–80,280, mainly distributed in Beijing, Shandong, Henan, Hubei, Sichuan, and the YRD and PRD regions. Gu et al. (2018) conducted a similar simulation for 2010, showing that $O_3$ caused approximately 271,000 premature mortalities and industrial sector was the most important contributor. Besides anthropogenic sources, Fu and Tai (2015) applied GEOS-Chem and found that climate change resulted in 2–10 ppb growth of summer $O_3$ in the most regions of East Asia and thereby about 6000 more premature deaths annually between 1980 and 2010. At the regional scale, Lu et al. (2016) estimated the health effect in PRD from 2010 to 2013 with WRF-CMAQ simulation and indicated that the four-year average of all-cause mortality associated with $O_3$ was 1271 for Guangzhou and the peak in premature mortality caused by $O_3$ occurred in March. Liu et al. (2020) applied WRF-CMAQ for Nanjing, and estimated that about 300 premature deaths (0.42–0.51 deaths per 10,000 people) were attributable to $O_3$ exposure throughout 2016. Regarding the health benefit of $O_3$ pollution control, Madaniyazi et al. (2016) designed two scenarios of "current legislation" and "maximum technically feasible reduction" based on the air pollution control in 2005. In the former scenario, the $O_3$-attributable premature death would increase over 40,000 in east China between 2005 and 2030, while up to 260,000 premature deaths would be avoided due to the restrained $O_3$ concentration in the latter. Zhang et al. (2020) applied WRF-CMAQ simulation and indicated that more than 1.5–2% of the emergency hospital admissions for cardiovascular and respiratory diseases resulting from $NO_2$ and $O_3$ exposure could be avoided in PRD, with a cooperative control strategy from 2015 to 2020.

$O_3$ is also harmful to vegetation due to its phytotoxicity when absorbed by leaf tissues, and a substantial reduction in crop yield and quality could be caused (Ashmore, 2005; Lin et al., 2018). Based on the simulated $O_3$ concentration with WRF-CMAQ, Qiao et al. (2019) reported a fraction of more than 75% of the forests over the country with $O_3$ exposure higher than the threshold of foliar injuries for 2013. Mills et al. (2018) evaluated the global ozone-induced crop production losses with the model of European Monitoring and Evaluation Programme, Meteorological Synthesising Centre-West (EMEP MSC-W), and China was found to be one of the countries suffered most severely from wheat rice and maize losses. Tang et al. (2013) conducted $O_3$ simulation with WRF-Chem and evaluated $O_3$-induced wheat production loss in China. They estimated that the relative wheat yield loss in 2000 was 6.4–14.9% and would increase by 8.1–9.4% in 2020. Miao et al. (2017) quantified the national crop yield losses due to $O_3$ exposure at 9.0, 4.6, 0.44 and 0.34 million metric tons for wheat, rice, maize and soybean for 2006, respectively. Lin et al. (2018) applied WRF-CMAQ and calculated a national production loss from all crops at 78.4 million metric tons caused by $O_3$ exposure for 2014.

In general, AQM simulations revealed that China's high and continuously increasing $O_3$ level resulted in harmful effects on human health and vegetation for the past decades. It should be noted that the uncertainty in the simulated $O_3$ concentration would be passed to the impact analysis, thus the evaluation of model performance should be emphasized when interpreting the impact of $O_3$ pollution based on AQM.

#### 4.3.2. The effectiveness of emission control and climate policies

AQM simulations help evaluate the effectiveness of emission control measures. Under the NAPPCAP since 2013, the toughest-ever clean air policy in China, the $NO_X$ emissions have declined sharply for the target of reducing $PM_{2.5}$ concentration (Chu et al., 2020; Zhang et al., 2019). The annual average $O_3$ concentration was simulated to increase by 12% over eastern China from 2012 to 2017 with GEOS-Chem, and the growth rates were 0.58 and 1.74 ppb $yr^{-1}$ for summer MDA8 $O_3$ in NCP and YRD, respectively (Dang and Liao, 2019; Dang et al., 2021). Based on WRF-CMAQ simulation, Liu and Wang (2020a) showed a similar result that the MDA8 $O_3$ in urban areas increased by 0.46 ppb $yr^{-1}$ from 2013 to 2017. In contrast, in rural areas with much fewer monitoring stations, MDA8 $O_3$ was simulated to decline slightly by 0.17 ppb $yr^{-1}$, resulting mainly from the $NO_X$ emission reduction under the $NO_X$-limit regime. The continuous growth of $O_3$ required more stringent measures of anthropogenic VOCs emission control in the future policy making. At the regional scale, Yu et al. (2019) applied WRF-CMAQ to assess the effect of emission reduction during 2014–2016 for PRD, and the $O_3$ was simulated to be reduced by 12.0 μg $m^{-3}$ (7.7%) in central Guangzhou.

Short-term measures for air quality improvement were conducted for important events, providing a good opportunity to explore the maximum reduction potential of $O_3$ pollution. With MM5-CMAQ simulation, Xing et al. (2011b) found a 47% and 57% reduction of $NO_X$ and non-methane VOCs emissions respectively within Beijing during the 2008 Olympics, resulting in a decline of DM1 $O_3$ concentration by −11%. However, the emission control strategy, with a 42% and 40% reduction of $NO_X$ and VOCs respectively, was less effective on $O_3$ pollution alleviation in PRD during the 2010 Asian Games (Liu et al., 2013). Guo et al. (2016) investigated the different impacts between joint and separate emission control measures during the Asia-Pacific Economic Cooperation (APEC) summit in 2014 with WRF-Chem. Compared to the uncontrolled scenario, they found a 41% growth of the simulated $O_3$ concentration (from 15.9 to 22.4 μg $m^{-3}$) due to the $NO_X$ emission

control for $PM_{2.5}$ reduction. A smaller growth of 1.5%, representing the effect of local emission control, was estimated with WRF-CMAQ simulations for the 2014 Youth Olympic Games in Nanjing (Huang et al., 2017). The situation seemed to be improved by the control strategy during the campaign of 2016 G20 summit, but the $O_3$ concentration remained high and the reduction was still smaller than other pollutants (Ni et al., 2020). To examine the effectiveness of the control measures during G20 summit, Wang and Liao (2020) conducted a series of sensitivity experiments with GEOS-Chem and found a reduction in MDA8 $O_3$ in Hangzhou by 6.8%, 8.9%, and 11.7% resulting from the implementation of control measures in the core area, Zhejiang province, and the whole YRD, respectively.

To design more effective policies of precursor emission control, AQMs were applied to examine the $O_3$ response to different VOCs/$NO_X$ emission reduction schemes. Lou et al. (2010) conducted a series of GEOS-Chem simulations and concluded that reduction of anthropogenic VOCs (AVOCs), both BVOCs and AVOCs, and both $NO_X$ and VOCs would be effective in eastern-northern, eastern-central and eastern-southern China, respectively. With the response surface methodology (RSM) based on CMAQ modeling for July 2005, Xing et al. (2011a) revealed that $NO_X$ control was more effective than VOCs control for reducing $O_3$ episodes for the megacities of Beijing, Shanghai and Guangzhou. Xu et al. (2019) implied that the downtown Shanghai would likely change into the transitional regime and other areas to $NO_X$-limited regime after 2020 if a further 20% reduction in $NO_X$ emissions could be achieved compared to 2015. For a manufacturing city in PRD, Foshan, Chen et al. (2019) conducted WRF-CMAQ simulations for different emission scenarios based on the situation in October 2015, to determine the $O_3$ response to precursor emission reduction in the VOC-limited region. They found that the VOCs to $NO_X$ emission abatement ratio greater than 1:1 would help effectively reduce $O_3$ concentration without increasing the $NO_2$ level. Based on the $O_3$ isopleth in 2010, however, Ou et al. (2016) indicated that $NO_X$ controls would be more promising in reaching $O_3$ attainment in a long term when $NO_X$-limited occupied in urban PRD, while AVOCs control was more efficient for reducing the peak $O_3$ level in a short term. Besides the eastern developed regions, studies have also been conducted for inland cities suffering severe $O_3$ pollution. Sun et al. (2021) suggested a transitional regime of summer $O_3$ formation for Luoyang, a city in the western edge of NCP, by plotting the $O_3$ isopleth with WRF-Chem simulation. They found that $NO_X$ reduction only would not decrease $O_3$ level until the emissions were cut down by 45%. When the ratio of reduced AVOCs to $NO_X$ mass concentration reached 3:1, the best $O_3$ control effect would be achieved. Li et al. (2020a) conducted WRF-Chem simulation with a series of emission control scenarios for Lanzhou, the largest industrialized city in northwest China, and found that VOCs control was more effective on $O_3$ pollution alleviation than $NO_X$ control.

Forecasting future $O_3$ level under different scenarios projected by Intergovernmental Panel on Climate Change (IPCC) could reveal the influence of climate change and human response on surface $O_3$ and guide policy making to overcome the climate penalty (Racherla and Adams, 2006; Wu et al., 2008). Zhu and Liao (2016) conducted a series of GEOS-Chem simulations for 2000–2050 under the Representative Concentration Pathways (RCPs, Moss et al., 2010) to evaluate the effect of emission changes on $O_3$ over the polluted regions. The average number of days with MDA8 $O_3$ exceeding 74.7 ppb was 3 for the four developed regions (NCP, YRD, PRD, and SCB) in 2000, while it would increase to 48 and 103 in 2030 and 2050, respectively, under RCP 6.0 emission scenario and the meteorological field of 2010. Similarly, Wang et al. (2021d) quantified the impact of future emission change on national $O_3$ level, and the relative changes between 2010 and 2050 would range from −13.3% to 3.7% for different RCP scenarios. Wang et al. (2013) found that climate change would increase $O_3$ concentration in eastern China but decrease in the west, under the IPCC A1B scenario with GEOS-Chem simulation for 2000 and 2050. Based on the IPCC Special Report Emissions Scenarios (SRES, Nakicenovic et al., 2000), Lee et al. (2015) applied CMAQ and identified the emission change as a key factor of future surface $O_3$ level for China. In contrast, the $O_3$ would be more greatly influenced by climate change in the developed country Japan. Besides, the influences of enhanced natural emissions and changed weather conditions have also been evaluated, by means of downscaling the results of global model as initial and boundary conditions for meteorological fields. Liu et al. (2019b) found that the climate-driven BVOCs changes under the RCP 8.5 scenario would enhance $O_3$ by 0.9% in eastern China in the 2050s compared to 2015, and the enhancement would account for 32% of the total $O_3$ changes. Xie et al. (2017) conducted a similar study for YRD with WRF-CALGRID model under IPCC A1B scenario between 2008 and 2050. They found that the variation of meteorological fields could significantly alter the spatial distribution of $O_3$, with a change of 5–15 ppb and −5 to −15 ppb in the north and south YRD, respectively. Moreover, the changes in BVOCs and soil $NO_X$ would account only for approximately 20% of the surface $O_3$ change caused by climate change. Hong et al. (2019) reported that climate would increase population-weighted average $O_3$ concentration by 4% and then lead to an additional 8900 death under RCP4.5 in 2050. The growth in $O_3$ and health exposure calls for more strict control policies to offset the climate penalty. Fig. 7 illustrates the projection of future $O_3$ level changes by various AQM studies. In general, the emission changes were predicted to enhance $O_3$ level under RCP scenarios with high temperature growth, but to restrain it under more stringent climate scenarios. The results emphasized that aggressive actions against climate warming will bring co-benefits to ozone pollution control.

To summarize, with an improved understanding on the mechanism of $O_3$ production, both the long-term and short-term policies on $O_3$ alleviation have gradually taken effect detected by AQM, despite the $NO_X$-focused strategy increased the $O_3$ level in VOC-limited regions. In the future, VOCs control should be emphasized and the negative effect of climate change should be taken into consideration for policy making.

## 5. Conclusion

This paper reviews the AQM performance and application of $O_3$ simulation in China. The major conclusions are summarized as below.

(1) AQMs provided a satisfactory capability in capturing the $O_3$ concentration and its variation in China, with the correlation coefficients over 0.5 and NMBs within ±30% in most of the reviewed studies, compared with available observations. Emission input, domain settings and model mechanisms played great roles on the AQM performance. For single-domain simulations, the best performance was found at the horizontal resolution of 12–30 km, while it would be improved at finer resolution in nested-domain simulations that applied regional models and refined local emission data. Given varied physical and chemical mechanisms built in models, overestimation in $O_3$ level was commonly provided by GEOS-Chem and CAMx, while the bias was less conclusive for WRF-Chem, CMAQ and NAQPMS. The efforts for further improvement of model performance contained the parameterized settings of surface schemes and inclusions of chloride reactions with nitrogen species and heterogeneous reactions on aerosols.

(2) AQMs were applied to identify the driving forces of $O_3$ growth, factors and processes for $O_3$ pollution episode, and the interactions with aerosols. The changes in anthropogenic emissions were expected to dominate the long-term $O_3$ growth in China, while meteorological conditions got increasingly important along with recent emission controls. High temperature, low relative humidity, strong vertical transportation and photochemical production were diagnosed as the main contributors to the short-term $O_3$ episodes. The suppression effect of $PM_{2.5}$ on $O_3$ formation included aerosol radiation feedback and heterogeneous

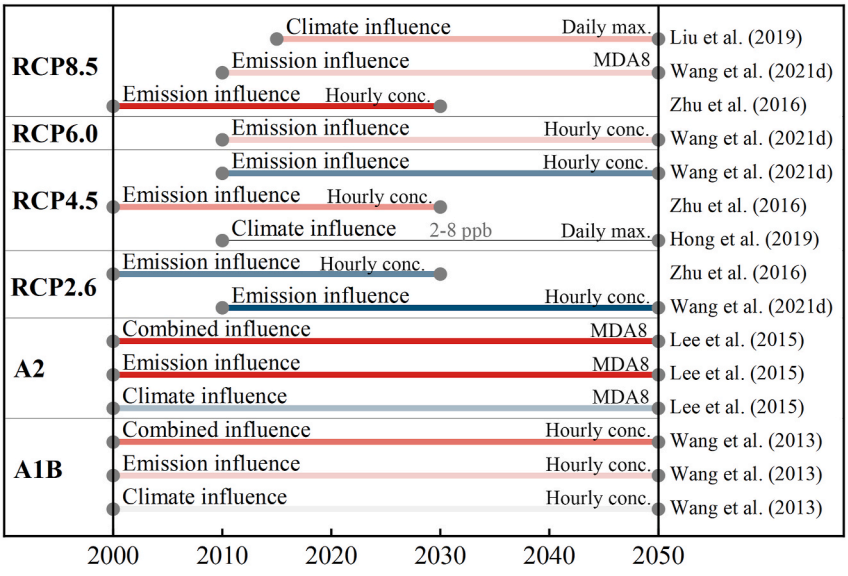


**Fig. 7.** Summary of the projections of future $O_3$ level changes under different climate scenarios. The endpoints of each line represent the starting and end years of the simulation, and the color represent the concentration changes between the two years. Marked on the upper left of the line are the influential factors of $O_3$ change, and marked on the upper right are the metrics used for $O_3$ concentration change. (For interpretation of the references to color in this figure legend, the reader is referred to the Web version of this article.)

uptake of gases and radicals, and has been weakened along with reduced aerosol pollution.

(3) AQMs were applied to explore the source-receptor relationship of $O_3$. In general, industry, transportation, and biogenic sources accounted collectively for 80% of $O_3$ and power contributed about 10%. For the four developed regions, industry was estimated to contribute most in the NCP, YRD and SCB regions, while transportation was more important in PRD. Local emissions were analyzed to account for only 30% of $O_3$ formation in several megacities, emphasizing the importance of regional transport and joint prevention and control of $O_3$. With various AQM techniques, a shift from VOC-limited to transitional regime has been detected in heavily polluted areas of eastern China, benefiting from the sharp reduction of $NO_X$ emissions.

(4) The AQM-derived $O_3$ concentration data with large spatiotemporal coverage supported environmental impact analysis and policy effectiveness evaluation. In the past two decades, China has experienced high and continuously increasing $O_3$ level, which in turn resulted in human health and vegetation damage. The annual deaths of tens of thousands were estimated attributed to the $O_3$ exposure. Both the long-term and short-term policies have gradually taken effect in limiting $O_3$ while reduction in $NO_X$ emissions has elevated the $O_3$ level in VOC-limited regions. In the future, more efforts should be conducted to control VOCs emissions along with continuous abatement of $NO_X$. Attentions should also be paid to restraining the rising $O_3$ levels caused by global warming.

Based on the reviews, recommendations are provided for simulating ozone in China. First, the quality of AQM input should be ensured. For example, the meteorology conditions need to be well predicted, especially temperature, relative humidity and wind speed. Local emission inventory with high horizontal resolution and accurate temporal variation is a better choice at regional and city scale, instead of downscaling the large scale emission inventories. Improvement on biogenic VOCs and soil $NO_X$ emissions also helps for warm seasons. Second, proper model resolution and initial and boundary conditions should be chosen. For national simulation, we recommend that the grid width to be around 30 km and the initial and boundary chemical conditions from the output of global chemical transport models, instead of clean air. For regional and city scale simulation, the inner domain of 9–15 km with 2 nest domains and inner domain of smaller than 5 km with 3–4 nest domains are more suitable respectively. Third, updating the chemical mechanisms in the model is encouraged in response to the changing atmospheric environment. For example, adding new heterogeneous chemical reactions and updating radical uptake coefficients will be beneficial, as the reduced $PM_{2.5}$ concentration may have raised $O_3$ level recently.

Furthermore, unresolved issues still exist in developing local photochemical indicator thresholds to better capture $O_3$ formation sensitivity shift for policy making, and diagnosing how $O_3$ will respond to climate change and emission reduction in the future. In addition, future efforts on $O_3$ modeling improvement should focus on developing emission inventories with dynamic and accurate information, applying halogen emissions into model, and adding or revising chemical schemes with updated observation information on OH reactions and VOCs oxidizations.

## Declaration of competing interest

The authors declare that they have no known competing financial interests or personal relationships that could have appeared to influence the work reported in this paper.

## Data availability

Data will be made available on request.

## Acknowledgement

This work was sponsored by the National Natural Science Foundation of China (41922052 and 42177080). We would also like to thank Prof. Jia Xing at Tsinghua University and Dr. Shovan Kumar Sahu for their comments on the paper.

## References

Ashmore, M.R., 2005. Assessing the future global impacts of ozone on vegetation. Plant Cell Environ. 28, 949–964. https://doi.org/10.1111/j.1365-3040.2005.01341.x.

Atkinson, R., 2000. Atmospheric chemistry of VOCs and NOx. Atmos. Environ. 34, 2063–2101. https://doi.org/10.1016/S1352-2310(99)00460-4.

Avnery, S., Mauzerall, D.L., Liu, J., Horowitz, L.W., 2011. Global crop yield reductions due to surface ozone exposure: 1. Year 2000 crop production losses and economic damage. Atmos. Environ. 45, 2284–2296. https://doi.org/10.1016/j.atmosenv.2010.11.045.

Brasseur, G.P., Jacob, D.J., 2017. Modeling of Atmospheric Chemistry. Cambridge University Press, Cambridge. https://doi.org/10.1017/9781316544754.

Carmichael, G.R., Sandu, A., Chai, T.F., Daescu, D.N., Constantinescu, E.M., Tang, Y.H., 2008. Predicting air quality: current status and future directions. In: Air Pollution

Modeling and its Application XIX, pp. 481–495. https://doi.org/10.1007/978-1-4020-8453-9_53.
Chen, X., Situ, S., Zhang, Q., Wang, X., Sha, C., Zhouc, L., Wu, L., Wu, L., Ye, L., Li, C., 2019. The synergetic control of NO2 and O3 concentrations in a manufacturing city of southern China. Atmos. Environ. 201, 402–416. https://doi.org/10.1016/j.atmosenv.2018.12.021.
Chu, B., Ma, Q., Liu, J., Ma, J., Zhang, P., Chen, T., Feng, Q., Wang, C., Yang, N., Ma, H., Ma, J., Russell, A.G., He, H., 2020. Air pollutant correlations in China: secondary air pollutant responses to NOx and SO2 control. Environ. Sci. Technol. Lett. 7, 695–700. https://doi.org/10.1021/acs.estlett.0c00403.
Cohan, D.S., Hakami, A., Hu, Y.T., Russell, A.G., 2005. Nonlinear response of ozone to emissions: source apportionment and sensitivity analysis. Environ. Sci. Technol. 39, 6739–6748. https://doi.org/10.1021/es048664m.
Colette, A., Granier, C., Hodnebrog, Ø., Jakobs, H., Maurizi, A., Nyiri, A., Bessagnet, B., D'Angiola, A., D'Isidoro, M., Gauss, M., Meleux, F., Memmesheimer, M., Mieville, A., Rouïl, L., Russo, F., Solberg, S., Stordal, F., Tampieri, F., 2011. Air quality trends in Europe over the past decade: a first multi-model assessment. Atmos. Chem. Phys. 11, 11657–11678. https://doi.org/10.5194/acp-11-11657-2011.
Dang, R., Liao, H., 2019. Radiative forcing and health impact of aerosols and ozone in China as the consequence of clean air actions over 2012-2017. Geophys. Res. Lett. 46, 12511–12519. https://doi.org/10.1029/2019gl084605.
Dang, R., Liao, H., Fu, Y., 2021. Quantifying the anthropogenic and meteorological influences on summertime surface ozone in China over 2012-2017. Sci. Total Environ. 754 https://doi.org/10.1016/j.scitotenv.2020.142394.
Deng, T., Chen, Y., Wan, Q., Zhang, Y., Deng, X., Huang, Y., Dai, G., Li, F., 2018. Comparative evaluation of the impact of GRAPES and MM5 meteorology on CMAQ prediction over Pearl River Delta, China. Particuology 40, 88–97. https://doi.org/10.1016/j.partic.2017.10.005.
Derwent, R.G., Collins, W.J., Johnson, C.E., Stevenson, D.S., 2001. Transient behaviour of tropospheric ozone precursors in a global 3-D CTM and their indirect greenhouse effects. Clim. Change 49, 463–487. https://doi.org/10.1023/a:1010648913655.
Ding, A.J., Huang, X., Nie, W., Sun, J.N., Kerminen, V.M., Petäjä, T., Su, H., Cheng, Y.F., Yang, X.Q., Wang, M.H., Chi, X.G., Wang, J.P., Virkkula, A., Guo, W.D., Yuan, J., Wang, S.Y., Zhang, R.J., Wu, Y.F., Song, Y., Zhu, T., Zilitinkevich, S., Kulmala, M., Fu, C.B., 2016. Enhanced haze pollution by black carbon in megacities in China. Geophys. Res. Lett. 43, 2873–2879. https://doi.org/10.1002/2016GL067745.
Ding, D., Xing, J., Wang, S.X., Chang, X., Hao, J.M., 2019. Impacts of emissions and meteorological changes on China's ozone pollution in the warm seasons of 2013 and 2017. Front. Environ. Sci. Eng. 13, 9. https://doi.org/10.1007/s11783-019-1160-1.
El-Harbawi, M., 2013. Air quality modelling, simulation, and computational methods: a review. Environ. Rev. 21, 149–179. https://doi.org/10.1139/er-2012-0056.
Emery, C., Liu, Z., Russell, A.G., Odman, M.T., Yarwood, G., Kumar, N., 2017. Recommendations on statistics and benchmarks to assess photochemical model performance. J. Air Waste Manag. Assoc. 67, 582–598. https://doi.org/10.1080/10962247.2016.1265027.
Emmerson, K.M., Evans, M.J., 2009. Comparison of tropospheric gas-phase chemistry schemes for use within global models. Atmos. Chem. Phys. 9, 1831–1845. https://doi.org/10.5194/acp-9-1831-2009.
Feng, T., Bei, N., Huang, R.J., Cao, J., Zhang, Q., Zhou, W., Tie, X., Liu, S., Zhang, T., Su, X., Lei, W., Molina, L.T., Li, G., 2016. Summertime ozone formation in Xi'an and surrounding areas, China, Atmos. Chem. Phys. 16, 4323–4342. https://doi.org/10.5194/acp-16-4323-2016.
Feng, T., Zhao, S., Bei, N., Wu, J., Liu, S., Li, X., Liu, L., Qian, Y., Yang, Q., Wang, Y., Zhou, W., Cao, J., Li, G., 2019. Secondary organic aerosol enhanced by increasing atmospheric oxidizing capacity in Beijing-Tianjin-Hebei (BTH), China, Atmos. Chem. Phys. 19, 7429–7443. https://doi.org/10.5194/acp-19-7429-2019.
Feng, X., Lin, H.P., Fu, T.M., Sulprizio, M.P., Zhuang, J.W., Jacob, D.J., Tian, H., Ma, Y. P., Zhang, L.J., Wang, X.L., Chen, Q., Han, Z.W., 2021. WRF-GC (v2.0): online two-way coupling of WRF (v3.9.1.1) and GEOS-Chem (v12.7.2) for modeling regional atmospheric chemistry-meteorology interactions. Geosci. Model Dev. (GMD) 14, 3741–3768. https://doi.org/10.5194/gmd-14-3741-2021.
FinlaysonPitts, B.J., Pitts, J.N., 1997. Tropospheric air pollution: ozone, airborne toxics, polycyclic aromatic hydrocarbons, and particles. Science 276, 1045–1052. https://doi.org/10.1126/science.276.5315.1045.
Fu, J.S., Hsu, N.C., Gao, Y., Huang, K., Li, C., Lin, N.H., Tsay, S.C., 2012. Evaluating the influences of biomass burning during 2006 BASE-ASIA: a regional chemical transport modeling. Atmos. Chem. Phys. 12, 3837–3855. https://doi.org/10.5194/acp-12-3837-2012.
Fu, X., Wang, T., Wang, S., Zhang, L., Cai, S., Xing, J., Hao, J., 2018. Anthropogenic emissions of hydrogen chloride and fine particulate chloride in China. Environ. Sci. Technol. 52, 1644–1654. https://doi.org/10.1021/acs.est.7b05030.
Fu, Y., Liao, H., 2014. Impacts of land use and land cover changes on biogenic emissions of volatile organic compounds in China from the late 1980s to the mid-2000s: implications for tropospheric ozone and secondary organic aerosol. Tellus Ser. B Chem. Phys. Meteorol. 66, 17. https://doi.org/10.3402/tellusb.v66.24987.
Fu, Y., Tai, A.P.K., 2015. Impact of climate and land cover changes on tropospheric ozone air quality and public health in East Asia between 1980 and 2010. Atmos. Chem. Phys. 15, 10093–10106. https://doi.org/10.5194/acp-15-10093-2015.
Fu, Y., Liao, H., Yang, Y., 2019. Interannual and decadal changes in tropospheric ozone in China and the associated chemistry-climate interactions: a review. Adv. Atmos. Sci. 36, 975–993. https://doi.org/10.1007/s00376-019-8216-9.
Gan, C.M., Hogrefe, C., Mathur, R., Pleim, J., Xing, J., Wong, D., Gilliam, R., Pouliot, G., Wei, C., 2016. Assessment of the effects of horizontal grid resolution on long-term air quality trends using coupled WRF-CMAQ simulations. Atmos. Environ. 132, 207–216. https://doi.org/10.1016/j.atmosenv.2016.02.036.
Gao, J., Zhu, B., Xiao, H., Kang, H., Hou, X., Shao, P., 2016. A case study of surface ozone source apportionment during a high concentration episode, under frequent shifting wind conditions over the Yangtze River Delta, China, Sci. Total Environ 544, 853–863. https://doi.org/10.1016/j.scitotenv.2015.12.039.
Gao, J., Zhu, B., Xiao, H., Kang, H., Pan, C., Wang, D., Wang, H., 2018. Effects of black carbon and boundary layer interaction on surface ozone in Nanjing, China, Atmos. Chem. Phys. 18, 7081–7094. https://doi.org/10.5194/acp-18-7081-2018.
Gao, J., Li, Y., Zhu, B., Hu, B., Wang, L., Bao, F., 2020a. What have we missed when studying the impact of aerosols on surface ozone via changing photolysis rates? Atmos. Chem. Phys. 20, 10831–10844. https://doi.org/10.5194/acp-20-10831-2020.
Gao, M., Gao, J., Zhu, B., Kumar, R., Lu, X., Song, S., Zhang, Y., Jia, B., Wang, P., Beig, G., Hu, J., Ying, Q., Zhang, H., Sherman, P., McElroy, M.B., 2020b. Ozone pollution over China and India: seasonality and sources. Atmos. Chem. Phys. 20, 4399–4414. https://doi.org/10.5194/acp-20-4399-2020.
Gong, C., Liao, H., 2019. A typical weather pattern for ozone pollution events in North China, Atmos. Chem. Phys. 19, 13725–13740. https://doi.org/10.5194/acp-19-13725-2019.
Gryparis, A., Forsberg, B., Katsouyanni, K., Analitis, A., Touloumi, G., Schwartz, J., Samoli, E., Medina, S., Anderson, H.R., Niciu, E.M., Wichmann, H.E., Kriz, B., Kosnik, M., Skorkovsky, J., Vonk, J.M., Dortbudak, Z., 2004. Acute effects of ozone on mortality from the "air pollution and health: a European approach" project. Am. J. Respir. Crit. Care Med. 170, 1080–1087. https://doi.org/10.1164/rccm.200403-333OC.
Gu, Y., Shu, J., 2010. The impact of urbanization on meteorological factors and ozone in Shanghai. Environmental Pollution & Control 32, 7–13 (in Chinese).
Gu, Y., Wong, T.W., Law, C.K., Dong, G.H., Ho, K.F., Yang, Y., Yim, S.H.L., 2018. Impacts of sectoral emissions in China and the implications: air quality, public health, crop production, and economic costs. Environ. Res. Lett. 13 https://doi.org/10.1088/1748-9326/aad138.
Guenther, A., Karl, T., Harley, P., Wiedinmyer, C., Palmer, P.I., Geron, C., 2006. Estimates of global terrestrial isoprene emissions using MEGAN (model of emissions of gases and aerosols from nature). Atmos. Chem. Phys. 6, 3181–3210. https://doi.org/10.5194/acp-6-3181-2006.
Guo, J., He, J., Liu, H., Miao, Y., Liu, H., Zhai, P., 2016. Impact of various emission control schemes on air quality using WRF-Chem during APEC China 2014. Atmos. Environ. 140, 311–319. https://doi.org/10.1016/j.atmosenv.2016.05.046.
Han, X., Zhu, L., Wang, S., Meng, X., Zhang, M., Hu, J., 2018. Modeling study of impacts on surface ozone of regional transport and emissions reductions over North China Plain in summer 2015. Atmos. Chem. Phys. 18, 12207–12221. https://doi.org/10.5194/acp-18-12207-2018.
Hogrefe, C., Biswas, J., Lynn, B., Civerolo, K., Ku, J.Y., Rosenthal, J., Rosenzweig, C., Goldberg, R., Kinney, P.L., 2004. Simulating regional-scale ozone climatology over the eastern United States: model evaluation results. Atmos. Environ. 38, 2627–2638. https://doi.org/10.1016/j.atmosenv.2004.02.033.
Hong, C., Zhang, Q., Zhang, Y., Davis, S.J., Tong, D., Zheng, Y., Liu, Z., Guan, D., He, K., Schellnhuber, H.J., 2019. Impacts of climate change on future air quality and human health in China. Proc. Natl. Acad. Sci. U. S. A 116, 17193–17200. https://doi.org/10.1073/pnas.1812881116.
Hong, Y., Liu, Y., Chen, X., Fan, Q., Chen, C., Chen, X., Wang, M., 2020. The role of anthropogenic chlorine emission in surface ozone formation during different seasons over eastern China. Sci. Total Environ. 723 https://doi.org/10.1016/j.scitotenv.2020.137697.
Hu, J., Chen, J., Ying, Q., Zhang, H., 2016. One-year simulation of ozone and particulate matter in China using WRF/CMAQ modeling system. Atmos. Chem. Phys. 16, 10333–10350. https://doi.org/10.5194/acp-16-10333-2016.
Hu, J., Li, X., Huang, L., Ying, Q., Zhang, Q., Zhao, B., Wang, S., Zhang, H., 2017. Ensemble prediction of air quality using the WRF/CMAQ model system for health effect studies in China. Atmos. Chem. Phys. 17, 13103–13118. https://doi.org/10.5194/acp-17-13103-2017.
Hu, J., Li, Y.C., Zhao, T.L., Liu, J., Hu, X.M., Liu, D.Y., Jiang, Y.C., Xu, J.M., Chang, L.Y., 2018. An important mechanism of regional O-3 transport for summer smog over the Yangtze River Delta in eastern China. Atmos. Chem. Phys. 18, 16239–16251. https://doi.org/10.5194/acp-18-16239-2018.
Huang, L., Zhu, Y., Zhai, H., Xue, S., Zhu, T., Shao, Y., Liu, Z., Emery, C., Yarwood, G., Wang, Y., Fu, J., Zhang, K., Li, L., 2021. Recommendations on benchmarks for numerical air quality model applications in China – Part 1: PM2.5 and chemical species. Atmos. Chem. Phys. 21, 2725–2743. https://doi.org/10.5194/acp-21-2725-2021.
Huang, Q., Wang, T., Chen, P., Huang, X., Zhu, J., Zhuang, B., 2017. Impacts of emission reduction and meteorological conditions on air quality improvement during the 2014 Youth Olympic Games in Nanjing, China, Atmos. Chem. Phys. 17, 13457–13471. https://doi.org/10.5194/acp-17-13457-2017.
Jacob, D.J., 2000. Heterogeneous chemistry and tropospheric ozone. Atmos. Environ. 34, 2131–2159. https://doi.org/10.1016/S1352-2310(99)00462-8.
Jacob, D.J., Winner, D.A., 2009. Effect of climate change on air quality. Atmos. Environ. 43, 51–63. https://doi.org/10.1016/j.atmosenv.2008.09.051.
Jeong, J.I., Park, R.J., 2013. Effects of the meteorological variability on regional air quality in East Asia. Atmos. Environ. 69, 46–55. https://doi.org/10.1016/j.atmosenv.2012.11.061.
Jerrett, M., Burnett, R.T., Pope 3rd, C.A., Ito, K., Thurston, G., Krewski, D., Shi, Y., Calle, E., Thun, M., 2009. Long-term ozone exposure and mortality. N. Engl. J. Med. 360, 1085–1095. https://doi.org/10.1056/NEJMoa0803894.
Jiang, X., Yoo, E.H., 2018. The importance of spatial resolutions of Community Multiscale Air Quality (CMAQ) models on health impact assessment. Sci. Total Environ. 627, 1528–1543. https://doi.org/10.1016/j.scitotenv.2018.01.228.

Jimenez, P., Baldasano, J.M., Dabdub, D., 2003. Comparison of photochemical mechanisms for air quality modeling. Atmos. Environ. 37, 4179–4194. https://doi.org/10.1016/S1352-2310(03)00567-3.

Jin, X., Holloway, T., 2015. Spatial and temporal variability of ozone sensitivity over China observed from the Ozone Monitoring Instrument. J. Geophys. Res. Atmos. 120, 7229–7246. https://doi.org/10.1002/2015jd023250.

Kwok, R.H.F., Baker, K.R., Napelenok, S.L., Tonnesen, G.S., 2015. Photochemical grid model implementation and application of VOC, NOx, and O3 source apportionment, Geosci. Model. Dev. 8, 99–114. https://doi.org/10.5194/gmd-8-99-2015.

Lee, H.M., Park, R.J., Henze, D.K., Lee, S., Shim, C., Shin, H.J., Moon, K.J., Woo, J.H., 2017. PM2.5 source attribution for Seoul in May from 2009 to 2013 using GEOS-Chem and its adjoint model. Environ. Pollut. 221, 377–384. https://doi.org/10.1016/j.envpol.2016.11.088.

Lee, J.B., Cha, J.S., Hong, S.C., Choi, J.Y., Myoung, J.S., Park, R.J., Woo, J.H., Ho, C., Han, J.S., Song, C.K., 2015. Projections of summertime ozone concentration over East Asia under multiple IPCC SRES emission scenarios. Atmos. Environ. 106, 335–346. https://doi.org/10.1016/j.atmosenv.2015.02.019.

Lei, H., Wuebbles, D.J., Liang, X.Z., 2012. Projected risk of high ozone episodes in 2050. Atmos. Environ. 59, 567–577. https://doi.org/10.1016/j.atmosenv.2012.05.051.

Li, G., Bei, N., Cao, J., Wu, J., Long, X., Feng, T., Dai, W., Liu, S., Zhang, Q., Tie, X., 2017. Widespread and persistent ozone pollution in eastern China during the non-winter season of 2015: observations and source attributions. Atmos. Chem. Phys. 17, 2759–2774. https://doi.org/10.5194/acp-17-2759-2017.

Li, M.M., Wang, T.J., Shu, L., Qu, Y.W., Xie, M., Liu, J.N., Wu, H., Kalsoom, U., 2021. Rising surface ozone in China from 2013 to 2017: A response to the recent atmospheric warming or pollutant controls? Atmos. Environ. 246, 118130 https://doi.org/10.1016/j.atmosenv.2020.118130.

Li, J., Wang, Z., Wang, X., Yamaji, K., Takigawa, M., Kanaya, Y., Pochanart, P., Liu, Y., Irie, H., Hu, B., Tanimoto, H., Akimoto, H., 2011. Impacts of aerosols on summertime tropospheric photolysis frequencies and photochemistry over Central Eastern China, Atmos. Environ. Times 45, 1817–1829. https://doi.org/10.1016/j.atmosenv.2011.01.016.

Li, J., Chen, X., Wang, Z., Du, H., Yang, W., Sun, Y., Hu, B., Li, J., Wang, W., Wang, T., Fu, P., Huang, H., 2018a. Radiative and heterogeneous chemical effects of aerosols on ozone and inorganic aerosols over East Asia. Sci. Total Environ. 622, 1327–1342. https://doi.org/10.1016/j.scitotenv.2017.12.041.

Li, J., Nagashima, T., Kong, L., Ge, B., Yamaji, K., Fu, J.S., Wang, X., Fan, Q., Itahashi, S., Lee, H.J., Kim, C.H., Lin, C.Y., Zhang, M., Tao, Z., Kajino, M., Liao, H., Li, M., Woo, J.-H., Kurokawa, J., Wang, Z., Wu, Q., Akimoto, H., Carmichael, G.R., Wang, Z., 2019a. Model evaluation and intercomparison of surface-level ozone and relevant species in East Asia in the context of MICS-Asia Phase III - Part 1: Overview. Atmos. Chem. Phys. 19, 12993–13015. https://doi.org/10.5194/acp-19-12993-2019.

Li, J., Wang, Z., Chen, L., Lian, L., Li, Y., Zhao, L., Zhou, S., Mao, X., Huang, T., Gao, H., Ma, J., 2020a. WRF-Chem simulations of ozone pollution and control strategy in petrochemical industrialized and heavily polluted Lanzhou City, Northwestern China. Sci. Total Environ. 737 https://doi.org/10.1016/j.scitotenv.2020.139835.

Li, K., Jacob, D.J., Liao, H., Shen, L., Zhang, Q., Bates, K.H., 2019b. Anthropogenic drivers of 2013-2017 trends in summer surface ozone in China. Proc. Natl. Acad. Sci. U. S. A 116, 422–427. https://doi.org/10.1073/pnas.1812168116.

Li, K., Jacob, D.J., Shen, L., Lu, X., De Smedt, I., Liao, H., 2020b. Increases in surface ozone pollution in China from 2013 to 2019: anthropogenic and meteorological influences. Atmos. Chem. Phys. 20, 11423–11433. https://doi.org/10.5194/acp-20-11423-2020.

Li, L., An, J.Y., Shi, Y.Y., Zhou, M., Yan, R.S., Huang, C., Wang, H.L., Lou, S.R., Wang, Q., Lu, Q., Wu, J., 2016a. Source apportionment of surface ozone in the Yangtze River delta, China in the summer of 2013, atmos. Environ. Times 144, 194–207. https://doi.org/10.1016/j.atmosenv.2016.08.076.

Li, L., An, J., Huang, L., Yan, R., Huang, C., Yarwood, G., 2019c. Ozone source apportionment over the Yangtze River Delta region, China: investigation of regional transport, sectoral contributions and seasonal differences. Atmos. Environ. 202, 269–280. https://doi.org/10.1016/j.atmosenv.2019.01.028.

Li, M., Song, Y., Mao, Z., Liu, M., Huang, X., 2016b. Impacts of thermal circulations induced by urbanization on ozone formation in the Pearl River Delta region, China, Atmos. Environ. Times 127, 382–392. https://doi.org/10.1016/j.atmosenv.2015.10.075.

Li, M.W., Wang, Y.X., Ju, W.M., 2014a. Effects of a remotely sensed land cover dataset with high spatial resolution on the simulation of secondary air pollutants over China using the nested-grid GEOS-chem chemical transport model. Adv. Atmos. Sci. 31, 179–187. https://doi.org/10.1007/s00376-013-2290-1.

Li, N., He, Q., Greenberg, J., Guenther, A., Li, J., Cao, J., Wang, J., Liao, H., Wang, Q., Zhang, Q., 2018b. Impacts of biogenic and anthropogenic emissions on summertime ozone formation in the Guanzhong Basin, China. Atmos. Chem. Phys. 18, 7489–7507. https://doi.org/10.5194/acp-18-7489-2018.

Li, Q., Zhang, L., Wang, T., Tham, Y.J., Ahmadov, R., Xue, L., Zhang, Q., Zheng, J., 2016c. Impacts of heterogeneous uptake of dinitrogen pentoxide and chlorine activation on ozone and reactive nitrogen partitioning: improvement and application of the WRF-Chem model in southern China. Atmos. Chem. Phys. 16, 14875–14890. https://doi.org/10.5194/acp-16-14875-2016.

Li, X.Y., Liu, J.F., Mauzerall, D.L., Emmons, L.K., Walters, S., Horowitz, L.W., Tao, S., 2014b. Effects of trans-Eurasian transport of air pollutants on surface ozone concentrations over Western China. J. Geophys. Res. Atmos. 119, 12338–12354. https://doi.org/10.1002/2014jd021936.

Li, Y., Lau, A.K.H., Fung, J.C.H., Zheng, J.Y., Zhong, L.J., Louie, P.K.K., 2012. Ozone source apportionment (OSAT) to differentiate local regional and super-regional source contributions in the Pearl River Delta region, China. J. Geophys. Res. Atmos. 117, 18. https://doi.org/10.1029/2011jd017340.

Li, Y., Lau, A.K.H., Fung, J.C.H., Ma, H., Tse, Y., 2013a. Systematic evaluation of ozone control policies using an Ozone Source Apportionment method. Atmos. Environ. 76, 136–146. https://doi.org/10.1016/j.atmosenv.2013.02.033.

Li, Y., Lau, A.K.H., Fung, J.C.H., Zheng, J.Y., Liu, S.C., 2013b. Importance of NOx control for peak ozone reduction in the Pearl River Delta region. J. Geophys. Res. Atmos. 118, 9428–9443. https://doi.org/10.1002/jgrd.50659.

Li, Q.Y., Zhang, L., Wang, T., Wang, Z., Fu, X., Zhang, Q., 2018c. New reactive nitrogen chemistry reshapes the relationship of ozone to its precursors. Environ. Sci. Technol. 52, 2810–2818. https://doi.org/10.1021/acs.est.7b05771.

Liang, Y., Yin, K., Hu, Y., Liu, B., Liao, R., Yan, M., 2014. Sensitivity analysis of ozone precursor emission in Shenzhen, China. China Environ. Sci. 34, 1390–1396.

Lin, Y., Jiang, F., Zhao, J., Zhu, G., He, X., Ma, X., Li, S., Sabel, C.E., Wang, H., 2018. Impacts of O3 on premature mortality and crop yield loss across China. Atmos. Environ. 194, 41–47. https://doi.org/10.1016/j.atmosenv.2018.09.024.

Liu, H., Wang, X.M., Zhang, J.P., He, K.B., Wu, Y., Xu, J.Y., 2013. Emission controls and changes in air quality in Guangzhou during the Asian Games. Atmos. Environ. 76, 81–93. https://doi.org/10.1016/j.atmosenv.2012.08.004.

Liu, H., Liu, S., Xue, B., Lv, Z., Meng, Z., Yang, X., Xue, T., Yu, Q., He, K., 2018a. Ground-level ozone pollution and its health impacts in China, Atmos. Environ. Times 173, 223–230. https://doi.org/10.1016/j.atmosenv.2017.11.014.

Liu, H., Zhang, M., Han, X., Li, J., Chen, L., 2019a. Episode analysis of regional contributions to tropospheric ozone in Beijing using a regional air quality model. Atmos. Environ. 199, 299–312. https://doi.org/10.1016/j.atmosenv.2018.11.044.

Liu, Q.X., Zhang, M.G., Wang, B., 2005. Simulation of tropospheric ozone with MOZART-2: an evaluation study over East Asia. Adv. Atmos. Sci. 22, 585–594. https://doi.org/10.1007/BF02918490.

Liu, S., Xing, J., Zhang, H., Ding, D., Zhang, F., Zhao, B., Sahu, S.K., Wang, S., 2019b. Climate-driven trends of biogenic volatile organic compound emissions and their impacts on summertime ozone and secondary organic aerosol in China in the 2050s. Atmos. Environ. 218 https://doi.org/10.1016/j.atmosenv.2019.117020.

Liu, T., Wang, C., Wang, Y., Huang, L., Li, J., Xie, F., Zhang, J., Hu, J., 2020. Impacts of model resolution on predictions of air quality and associated health exposure in Nanjing, China. Chemosphere 249. https://doi.org/10.1016/j.chemosphere.2020.126515.

Liu, X.H., Zhang, Y., Xing, J., Zhang, Q.A., Wang, K., Streets, D.G., Jang, C., Wang, W.X., Hao, J.M., 2010. Understanding of regional air pollution over China using CMAQ, part II. Process analysis and sensitivity of ozone and particulate matter to precursor emissions. Atmos. Environ. 44, 3719–3727. https://doi.org/10.1016/j.atmosenv.2010.03.036.

Liu, Y., Li, L., An, J., Huang, L., Yan, R., Huang, C., Wang, H., Wang, Q., Wang, M., Zhang, W., 2018b. Estimation of biogenic VOC emissions and its impact on ozone formation over the Yangtze River Delta region, China, Atmos. Environ. Times 186, 113–128. https://doi.org/10.1016/j.atmosenv.2018.05.027.

Liu, Y., Wang, T., 2020a. Worsening urban ozone pollution in China from 2013 to 2017-Part 1: the complex and varying roles of meteorology. Atmos. Chem. Phys. 20, 6305–6321. https://doi.org/10.5194/acp-20-6305-2020.

Liu, Y., Wang, T., 2020b. Worsening urban ozone pollution in China from 2013 to 2017-Part 2: the effects of emission changes and implications for multi-pollutant control. Atmos. Chem. Phys. 20, 6323–6337. https://doi.org/10.5194/acp-20-6323-2020.

Lou, S., Zhu, B., Liao, H., 2010. Lmpacts of O3 precursor on surface O3 concentration over China. Transactions of Atmospheric Sciences (in Chinese) 33, 451–459.

Lou, S., Liao, H., Yang, Y., Mu, Q., 2015. Simulation of the interannual variations of tropospheric ozone over China: roles of variations in meteorological parameters and anthropogenic emissions. Atmos. Environ. 122, 839–851. https://doi.org/10.1016/j.atmosenv.2015.08.081.

Lou, S.J., Liao, H., Zhu, B., 2014. Impacts of aerosols on surface-layer ozone concentrations in China through heterogeneous reactions and changes in photolysis rates. Atmos. Environ. 85, 123–138. https://doi.org/10.1016/j.atmosenv.2013.12.004.

Lu, X., Yao, T., Fung, J.C.H., Lin, C., 2016. Estimation of health and economic costs of air pollution over the Pearl River Delta region in China. Sci. Total Environ. 566, 134–143. https://doi.org/10.1016/j.scitotenv.2016.05.060.

Lu, X., Hong, J., Zhang, L., Cooper, O.R., Schultz, M.G., Xu, X., Wang, T., Gao, M., Zhao, Y., Zhang, Y., 2018. Severe surface ozone pollution in China: a global perspective. Environ. Sci. Technol. Lett. 5, 487–494. https://doi.org/10.1021/acs.estlett.8b00366.

Lu, X., Zhang, L., Chen, Y., Zhou, M., Zheng, B., Li, K., Liu, Y., Lin, J., Fu, T.M., Zhang, Q., 2019a. Exploring 2016-2017 surface ozone pollution over China: source contributions and meteorological influences. Atmos. Chem. Phys. 19, 8339–8361. https://doi.org/10.5194/acp-19-8339-2019.

Lu, X., Zhang, L., Shen, L., 2019b. Meteorology and climate influences on tropospheric ozone: a review of natural sources, chemistry, and transport patterns. Curr. Pollut. Rep. 5, 238–260. https://doi.org/10.1007/s40726-019-00118-3.

Lu, X., Ye, X., Zhou, M., Zhao, Y., Weng, H., Kong, H., Li, K., Gao, M., Zheng, B., Lin, J., Zhou, F., Zhang, Q., Wu, D., Zhang, L., Zhang, Y., 2021. The underappreciated role of agricultural soil nitrogen oxide emissions in ozone pollution regulation in North China. Nat. Commun. 12, 5021. https://doi.org/10.1038/s41467-021-25147-9.

Ma, J., van Aardenne, J.A., 2004. Impact of different emission inventories on simulated tropospheric ozone over China: a regional chemical transport model evaluation. Atmos. Chem. Phys. 4, 877–887. https://doi.org/10.5194/acp-4-877-2004.

Ma, M., Gao, Y., Wang, Y., Zhang, S., Leung, L.R., Liu, C., Wang, S., Zhao, B., Chang, X., Su, H., Zhang, T., Sheng, L., Yao, X., Gao, H., 2019. Substantial ozone enhancement over the North China Plain from increased biogenic emissions due to heat waves and

land cover in summer 2017. Atmos. Chem. Phys. 19, 12195–12207. https://doi.org/10.5194/acp-19-12195-2019.
Madaniyazi, L., Nagashima, T., Guo, Y., Pan, X., Tong, S., 2016. Projecting ozone-related mortality in East China. Environ. Int. 92–93, 165–172. https://doi.org/10.1016/j.envint.2016.03.040.
Miao, W.J., Huang, X., Song, Y., 2017. An economic assessment of the health effects and crop yield losses caused by air pollution in mainland China. J. Environ. Sci. 56, 102–113. https://doi.org/10.1016/j.jes.2016.08.024.
Mills, G., Sharps, K., Simpson, D., Pleijel, H., Frei, M., Burkey, K., Emberson, L., Uddling, J., Broberg, M., Feng, Z.Z., Kobayashi, K., Agrawal, M., 2018. Closing the global ozone yield gap: quantification and cobenefits for multistress tolerance. Global Change Biol. 24, 4869–4893. https://doi.org/10.1111/gcb.14381.
Moss, R.H., Edmonds, J.A., Hibbard, K.A., Manning, M.R., Rose, S.K., van Vuuren, D.P., Carter, T.R., Emori, S., Kainuma, M., Kram, T., Meehl, G.A., Mitchell, J.F., Nakicenovic, N., Riahi, K., Smith, S.J., Stouffer, R.J., Thomson, A.M., Weyant, J.P., Wilbanks, T.J., 2010. The next generation of scenarios for climate change research and assessment. Nature 463, 747–756. https://doi.org/10.1038/nature08823.
Nakicenovic, N., Alcamo, J., Davis, G., Vries, B.D., 2000. Special Report on Emissions Scenarios: a Special Report of the Working Group III of the Intergovernmental Panel on Climate Change. Cambridge University Press, New York.
Ni, R., Lin, J., Yan, Y., Lin, W., 2018. Foreign and domestic contributions to springtime ozone over China. Atmos. Chem. Phys. 18, 11447–11469. https://doi.org/10.5194/acp-18-11447-2018.
Ni, Z.Z., Luo, K., Gao, X., Gao, Y., Fan, J.R., Fu, J.S., Chen, C.H., 2019. Exploring the stratospheric source of ozone pollution over China during the 2016 Group of Twenty summit. Atmos. Pollut. Res. 10, 1267–1275. https://doi.org/10.1016/j.apr.2019.02.010.
Ni, Z.Z., Luo, K., Gao, Y., Gao, X., Jiang, F., Huang, C., Fan, J.R., Fu, J.S., Chen, C.H., 2020. Spatial-temporal variations and process analysis of O-3 pollution in Hangzhou during the G20 summit. Atmos. Chem. Phys. 20, 5963–5976. https://doi.org/10.5194/acp-20-5963-2020.
Ou, J., Yuan, Z., Zheng, J., Huang, Z., Shao, M., Li, Z., Huang, X., Guo, H., Louie, P.K., 2016. Ambient ozone control in a photochemically active region: short-term despiking or long-term attainment? Environ. Sci. Technol. 50, 5720–5728. https://doi.org/10.1021/acs.est.6b00345.
Park, R.J., Kim, S.W., 2014. Air quality modeling in East Asia: present issues and future directions, Asia Pac. J. Atmos. Sci. 50, 105–120. https://doi.org/10.1007/s13143-014-0030-9.
Pu, X., Wang, T.J., Huang, X., Melas, D., Zanis, P., Papanastasiou, D.K., Poupkou, A., 2017. Enhanced surface ozone during the heat wave of 2013 in Yangtze River Delta region, China, Sci. Total Environ 603, 807–816. https://doi.org/10.1016/j.scitotenv.2017.03.056.
Qiao, X., Wang, P., Zhang, J., Zhang, H., Tang, Y., Hu, J., Ying, Q., 2019. Spatial-temporal variations and source contributions to forest ozone exposure in China. Sci. Total Environ. 674, 189–199. https://doi.org/10.1016/j.scitotenv.2019.04.106.
Qiu, X., Ying, Q., Wang, S., Duan, L., Wang, Y., Lu, K., Wang, P., Xing, J., Zheng, M., Zhao, M., Zheng, H., Zhang, Y., Hao, J., 2019. Significant impact of heterogeneous reactions of reactive chlorine species on summertime atmospheric ozone and free-radical formation in north China, Sci. Total Environ 693. https://doi.org/10.1016/j.scitotenv.2019.133580.
Racherla, P.N., Adams, P.J., 2006. Sensitivity of global tropospheric ozone and fine particulate matter concentrations to climate change. J. Geophys. Res. Atmos. 111 https://doi.org/10.1029/2005jd006939.
Saikawa, E., Kim, H., Zhong, M., Avramov, A., Zhao, Y., Janssens-Maenhout, G., Kurokawa, J.-i., Klimont, Z., Wagner, F., Naik, V., Horowitz, L.W., Zhang, Q., 2017. Comparison of emissions inventories of anthropogenic air pollutants and greenhouse gases in China. Atmos. Chem. Phys. 17, 6393–6421. https://doi.org/10.5194/acp-17-6393-2017.
Seinfeld, H., Pandis, S., 1998. Atmospheric Chemistry and Physics, from Air Pollution to Climate Change. John Wiley & Sons.
Shao, M., Tang, X., Zhang, Y., Li, W., 2006. City clusters in China: air and surface water pollution. Front. Ecol. Environ. 4, 353–361. https://doi.org/10.1890/1540-9295(2006)004[0353:CCICAA]2.0.CO;2.
Sharma, S., Sharma, P., Khare, M., 2017. Photo-chemical transport modelling of tropospheric ozone: a review. Atmos. Environ. 159, 34–54. https://doi.org/10.1016/j.atmosenv.2017.03.047.
Shen, H.Z., Sun, Z., Chen, Y.L., Russell, A.G., Hu, Y.T., Odman, M.T., Qian, Y., Archibald, A.T., Tao, S., 2021. Novel method for ozone isopleth construction and diagnosis for the ozone control strategy of Chinese cities. Environ. Sci. Technol. 55, 15625–15636. https://doi.org/10.1021/acs.est.1c01567.
Shen, J., Wang, X.S., Li, J.F., Li, Y.P., Zhang, Y.H., 2011. Evaluation and intercomparison of ozone simulations by models-3/CMAQ and CAMx over the Pearl River delta. Sci. China Chem. 54, 1789–1800. https://doi.org/10.1007/s11426-011-4390-z.
Shu, L., Xie, M., Wang, T., Gao, D., Chen, P., Han, Y., Li, S., Zhuang, B., Li, M., 2016. Integrated studies of a regional ozone pollution synthetically affected by subtropical high and typhoon system in the Yangtze River Delta region, China, Atmos. Chem. Phys. 16, 15801–15819. https://doi.org/10.5194/acp-16-15801-2016.
Shu, L., Wang, T., Xie, M., Li, M., Zhao, M., Zhang, M., Zhao, X., 2019. Episode study of fine particle and ozone during the CAPUM-YRD over Yangtze River Delta of China: characteristics and source attribution, Atmos. Environ. Times 203, 87–101. https://doi.org/10.1016/j.atmosenv.2019.01.044.
Shu, L., Wang, T., Han, H., Xie, M., Chen, P., Li, M., Wu, H., 2020. Summertime ozone pollution in the Yangtze River Delta of eastern China during 2013-2017: synoptic impacts and source apportionment. Environ. Pollut. 257 https://doi.org/10.1016/j.envpol.2019.113631.
Sillman, S., 1995. The use of NOy, H2O2, and HNO3 as indicators for ozone-NOx-hydrocarbon sensitivity in urban locations. J. Geophys. Res. Atmos. 100, 14175–14188. https://doi.org/10.1029/94JD02953.
Sillman, S., He, D.Y., 2002. Some theoretical results concerning O-3-NOx-VOC chemistry and NOx-VOC indicators. J. Geophys. Res. Atmos. 107, 15. https://doi.org/10.1029/2001jd001123.
Sillman, S., West, J.J., 2009. Reactive nitrogen in Mexico City and its relation to ozone-precursor sensitivity: results from photochemical models. Atmos. Chem. Phys. 9, 3477–3489. https://doi.org/10.5194/acp-9-3477-2009.
Simpson, W.R., Brown, S.S., Saiz-Lopez, A., Thornton, J.A., von Glasow, R., 2015. Tropospheric halogen chemistry: sources, cycling, and impacts. Chem. Rev. 115, 4035–4062. https://doi.org/10.1021/cr5006638.
Situ, S., Guenther, A., Wang, X., Jiang, X., Turnipseed, A., Wu, Z., Bai, J., Wang, X., 2013. Impacts of seasonal and regional variability in biogenic VOC emissions on surface ozone in the Pearl River delta region, China. Atmos. Chem. Phys. 13, 11803–11817. https://doi.org/10.5194/acp-13-11803-2013.
Sokhi, R.S., San José, R., Kitwiroon, N., Fragkou, E., Pérez, J.L., Middleton, D.R., 2006. Prediction of ozone levels in London using the MM5-CMAQ modelling system. Environ. Model. Software 21, 566–576. https://doi.org/10.1016/j.envsoft.2004.07.016.
Solazzo, E., Bianconi, R., Hogrefe, C., Curci, G., Tuccella, P., Alyuz, U., Balzarini, A., Baró, R., Bellasio, R., Bieser, J., Brandt, J., Christensen, J.H., Colette, A., Francis, X., Fraser, A., Vivanco, M.G., Jiménez-Guerrero, P., Im, U., Manders, A., Nopmongcol, U., Kitwiroon, N., Pirovano, G., Pozzoli, L., Prank, M., Sokhi, R.S., Unal, A., Yarwood, G., Galmarini, S., 2017. Evaluation and error apportionment of an ensemble of atmospheric chemistry transport modeling systems: multivariable temporal and spatial breakdown. Atmos. Chem. Phys. 17, 3001–3054. https://doi.org/10.5194/acp-17-3001-2017.
Sun, J., Shen, Z., Wang, R., Li, G., Zhang, Y., Zhang, B., He, K., Tang, Z., Xu, H., Qu, L., Sai Hang Ho, S., Liu, S., Cao, J., 2021. A comprehensive study on ozone pollution in a megacity in North China Plain during summertime: observations, source attributions and ozone sensitivity. Environ. Int. 146 https://doi.org/10.1016/j.envint.2020.106279, 106279-106279.
Sun, L., Xue, L., Wang, Y., Li, L., Lin, J., Ni, R., Yan, Y., Chen, L., Li, J., Zhang, Q., Wang, W., 2019. Impacts of meteorology and emissions on summertime surface ozone increases over central eastern China between 2003 and 2015. Atmos. Chem. Phys. 19, 1455–1469. https://doi.org/10.5194/acp-19-1455-2019.
Tang, G., Zhu, X., Xin, J., Hu, B., Song, T., Sun, Y., Zhang, J., Wang, L., Cheng, M., Chao, N., Kong, L., Li, X., Wang, Y., 2017. Modelling study of boundary-layer ozone over northern China - Part I: ozone budget in summer. Atmos. Res. 187, 128–137. https://doi.org/10.1016/j.atmosres.2016.10.017.
Tang, H., Takigawa, M., Liu, G., Zhu, J., Kobayashi, K., 2013. A projection of ozone-induced wheat production loss in China and India for the years 2000 and 2020 with exposure-based and flux-based approaches. Global Change Biol. 19, 2739–2752. https://doi.org/10.1111/gcb.12252.
Tao, H., Xing, J., Zhou, H., Chang, X., Li, G., Chen, L., Li, J., 2018. Impacts of land use and land cover change on regional meteorology and air quality over the Beijing-Tianjin-Hebei region, China, Atmos. Environ. Times 189, 9–21. https://doi.org/10.1016/j.atmosenv.2018.06.033.
Tao, Z., Chin, M., Gao, M., Kucsera, T., Kim, D., Bian, H., Kurokawa, J., Wang, Y., Liu, Z., Carmichael, G.R., Wang, Z., Akimoto, H., 2020. Evaluation of NU-WRF model performance on air quality simulation under various model resolutions - an investigation within the framework of MICS-Asia Phase III. Atmos. Chem. Phys. 20, 2319–2339. https://doi.org/10.5194/acp-20-2319-2020.
Tonnesen, G.S., Dennis, R.L., 2000. Analysis of radical propagation efficiency to assess ozone sensitivity to hydrocarbons and NOx 2. Long-lived species as indicators of ozone concentration sensitivity. J. Geophys. Res. Atmos. 105, 9227–9241. https://doi.org/10.1029/1999JD900372.
USEPA, 2001. Guidance for demonstrating attainment of air quality goals for PM 2.5 and regional haze. draft 2, 1.
van Eck, N.J., Waltman, L., 2010. Software survey: VOSviewer, a computer program for bibliometric mapping. Scientometrics 84, 523–538. https://doi.org/10.1007/s11192-009-0146-3.
Wai, K.M., Tanner, P.A., 2010. Variations of aerosol properties due to regional source contributions and impacts on ozone levels: a study in a south China city. Environ. Chem. 7, 359–369. https://doi.org/10.1071/en10020.
Wang, H.L., Wu, K., Liu, Y.M., Sheng, B.S., Lu, X., He, Y.P., Xie, J.L., Wang, H.C., Fan, S.J., 2021a. Role of heat wave-induced biogenic VOC enhancements in persistent ozone episodes formation in Pearl River delta. J. Geophys. Res. Atmos. 126, 19. https://doi.org/10.1029/2020jd034317.
Wang, N., Lyu, X.P., Deng, X.J., Guo, H., Deng, T., Li, Y., Yin, C.Q., Li, F., Wang, S.Q., 2016. Assessment of regional air quality resulting from emission control in the Pearl River Delta region, southern China. Sci. Total Environ. 573, 1554–1565. https://doi.org/10.1016/j.scitotenv.2016.09.013.
Wang, N., Lyu, X., Deng, X., Huang, X., Jiang, F., Ding, A., 2019a. Aggravating O3 pollution due to NOx emission control in eastern China, Sci. Total Environ 677, 732–744. https://doi.org/10.1016/j.scitotenv.2019.04.388.
Wang, P., Chen, Y., Hu, J., Zhang, H., Ying, Q., 2019b. Attribution of tropospheric ozone to NOx and VOC emissions: considering ozone formation in the transition regime. Environ. Sci. Technol. 53, 1404–1412. https://doi.org/10.1021/acs.est.8b05981.
Wang, P., Chen, Y., Hu, J., Zhang, H., Ying, Q., 2019c. Source apportionment of summertime ozone in China using a source-oriented chemical transport model. Atmos. Environ. 211, 79–90. https://doi.org/10.1016/j.atmosenv.2019.05.006.
Wang, P., Guo, H., Hu, J., Kota, S.H., Ying, Q., Zhang, H., 2019d. Responses of PM2.5 and O3 concentrations to changes of meteorology and emissions in China. Sci. Total Environ. 662, 297–306. https://doi.org/10.1016/j.scitotenv.2019.01.227.

Wang, P., Qiao, X., Zhang, H., 2020a. Modeling PM2.5 and O-3 with aerosol feedbacks using WRF/Chem over the Sichuan Basin, southwestern China. Chemosphere 254. https://doi.org/10.1016/j.chemosphere.2020.126735.
Wang, R., Tie, X., Li, G., Zhao, S., Long, X., Johansson, L., An, Z., 2019e. Effect of ship emissions on O-3 in the Yangtze River delta region of China: analysis of WRF-chem modeling. Sci. Total Environ. 683, 360–370. https://doi.org/10.1016/j.scitotenv.2019.04.240.
Wang, T., Xue, L., Brimblecombe, P., Lam, Y.F., Li, L., Zhang, L., 2017. Ozone pollution in China: a review of concentrations, meteorological influences, chemical precursors, and effects. Sci. Total Environ. 575, 1582–1596. https://doi.org/10.1016/j.scitotenv.2016.10.081.
Wang, X., Zhang, Y., Hu, Y., Zhou, W., Lu, K., Zhong, L., Zeng, L., Shao, M., Hu, M., Russell, A.G., 2010. Process analysis and sensitivity study of regional ozone formation over the Pearl River Delta, China, during the PRIDE-PRD2004 campaign using the Community Multiscale Air Quality modeling system. Atmos. Chem. Phys. 10, 4423–4437. https://doi.org/10.5194/acp-10-4423-2010.
Wang, X., Jacob, D.J., Eastham, S.D., Sulprizio, M.P., Zhu, L., Chen, Q., Alexander, B., Sherwen, T., Evans, M.J., Lee, B.H., Haskins, J.D., Lopez-Hilfiker, F.D., Thornton, J. A., Huey, G.L., Liao, H., 2019f. The role of chlorine in global tropospheric chemistry. Atmos. Chem. Phys. 19, 3981–4003. https://doi.org/10.5194/acp-19-3981-2019.
Wang, X., Jacob, D.J., Fu, X., Wang, T., Le Breton, M., Hallquist, M., Liu, Z., McDuffie, E. E., Liao, H., 2020b. Effects of anthropogenic chlorine on PM2.5 and ozone air quality in China. Environ. Sci. Technol. 54, 9908–9916. https://doi.org/10.1021/acs.est.0c02296.
Wang, X., Fu, T.M., Zhang, L., Cao, H., Zhang, Q., Ma, H., Shen, L., Evans, M.J., Ivatt, P. D., Lu, X., Chen, Y., Zhang, L., Feng, X., Yang, X., Zhu, L., Henze, D.K., 2021b. Sensitivities of ozone air pollution in the beijing-tianjin-hebei area to local and upwind precursor emissions using adjoint modeling. Environ. Sci. Technol. 55, 5752–5762. https://doi.org/10.1021/acs.est.1c00131.
Wang, X.S., Zhang, Y.H., Hu, Y.T., Zhou, W., Zeng, L.M., Hu, M., Cohan, D.S., Russell, A. G., 2011a. Decoupled direct sensitivity analysis of regional ozone pollution over the Pearl River Delta during the PRIDE-PRD2004 campaign. Atmos. Environ. 45, 4941–4949. https://doi.org/10.1016/j.atmosenv.2011.06.006.
Wang, X.Y., Li, L., Gong, K.J., Mao, J.J., Hu, J.L., Li, J.Y., Liu, Z.X., Liao, H., Qiu, W.Y., Yu, Y., Dong, H.B., Guo, S., Hu, M., Zeng, L.M., Zhang, Y.H., 2021c. Modelling air quality during the EXPLORE-YRD campaign-Part I. Model performance evaluation and impacts of meteorological inputs and grid resolutions. Atmos. Environ. 246, 12. https://doi.org/10.1016/j.atmosenv.2020.118131.
Wang, Y., Zhang, Y., Hao, J., Luo, M., 2011b. Seasonal and spatial variability of surface ozone over China: contributions from background and domestic pollution. Atmos. Chem. Phys. 11, 3511–3525. https://doi.org/10.5194/acp-11-3511-2011.
Wang, Y., Liao, H., 2020. Effect of emission control measures on ozone concentrations in Hangzhou during G20 meeting in 2016. Chemosphere 261. https://doi.org/10.1016/j.chemosphere.2020.127729.
Wang, Y., Zhao, Y., Zhang, L., Zhang, J., Liu, Y., 2020c. Modified regional biogenic VOC emissions with actual ozone stress and integrated land cover information: a case study in Yangtze River Delta, China, Sci. Total Environ 727, 138703. https://doi.org/10.1016/j.scitotenv.2020.138703.
Wang, Y.L., Wild, O., Chen, X.S., Wu, Q.Z., Gao, M., Chen, H.S., Qi, Y., Wang, Z.F., 2020d. Health impacts of long-term ozone exposure in China over 2013-2017. Environ. Int. 144, 11. https://doi.org/10.1016/j.envint.2020.106030.
Wang, Y.X., Shen, L.L., Wu, S.L., Mickley, L., He, J.W., Hao, J.M., 2013. Sensitivity of surface ozone over China to 2000-2050 global changes of climate and emissions. Atmos. Environ. 75, 374–382. https://doi.org/10.1016/j.atmosenv.2013.04.045.
Wang, Y.Y., Hu, J.L., Zhu, J., Li, J.Y., Qin, M.M., Liao, H., Chen, K., Wang, M., 2021d. Health Burden and economic impacts attributed to PM2.5 and O-3 in China from 2010 to 2050 under different representative concentration pathway scenarios. Resour. Conserv. Recycl. 173, 8. https://doi.org/10.1016/j.resconrec.2021.105731.
Wei, W., Lv, Z.F., Li, Y., Wang, L.T., Cheng, S., Liu, H., 2018. A WRF-Chem model study of the impact of VOCs emission of a huge petrochemical industrial zone on the summertime ozone in Beijing, China, Atmos. Environ. Times 175, 44–53. https://doi.org/10.1016/j.atmosenv.2017.11.058.
Wei, W., Li, Y., Ren, Y., Cheng, S., Han, L., 2019. Sensitivity of summer ozone to precursor emission change over Beijing during 2010-2015: a WRF-Chem modeling study. Atmos. Environ. 218 https://doi.org/10.1016/j.atmosenv.2019.116984.
Wei, X.L., Liu, Q., Lam, K.S., Wang, T.J., 2012. Impact of precursor levels and global warming on peak ozone concentration in the Pearl River Delta Region of China. Adv. Atmos. Sci. 29, 635–645. https://doi.org/10.1007/s00376-011-1167-4.
Wild, O., Akimoto, H., 2001. Intercontinental transport of ozone and its precursors in a three-dimensional global CTM. J. Geophys. Res. Atmos. 106, 27729–27744. https://doi.org/10.1029/2000jd000123.
Wittig, V.E., Ainsworth, E.A., Naidu, S.L., Karnosky, D.F., Long, S.P., 2009. Quantifying the impact of current and future tropospheric ozone on tree biomass, growth, physiology and biochemistry: a quantitative meta-analysis. Global Change Biol. 15, 396–424. https://doi.org/10.1111/j.1365-2486.2008.01774.x.
Wu, J., Li, G., Cao, J., Bei, N., Wang, Y., Feng, T., Huang, R., Liu, S., Zhang, Q., Tie, X., 2017. Contributions of trans-boundary transport to summertime air quality in Beijing, China. Atmos. Chem. Phys. 17, 2035–2051. https://doi.org/10.5194/acp-17-2035-2017.
Wu, J., Bei, N., Li, X., Cao, J., Feng, T., Wang, Y., Tie, X., Li, G., 2018. Widespread air pollutants of the North China Plain during the Asian summer monsoon season: a case study. Atmos. Chem. Phys. 18, 8491–8504. https://doi.org/10.5194/acp-18-8491-2018.
Wu, K., Yang, X., Chen, D., Gu, S., Lu, Y., Jiang, Q., Wang, K., Ou, Y., Qian, Y., Shao, P., Lu, S., 2020. Estimation of biogenic VOC emissions and their corresponding impact on ozone and secondary organic aerosol formation in China. Atmos. Res. 231 https://doi.org/10.1016/j.atmosres.2019.104656.
Wu, S., Mickley, L.J., Jacob, D.J., Rind, D., Streets, D.G., 2008. Effects of 2000–2050 changes in climate and emissions on global tropospheric ozone and the policy-relevant background surface ozone in the United States. J. Geophys. Res. 113 https://doi.org/10.1029/2007jd009639.
Xie, M., Zhu, K.G., Wang, T.J., Yang, H.M., Zhuang, B.L., Li, S., Li, M.G., Zhu, X.S., Ouyang, Y., 2014. Application of photochemical indicators to evaluate ozone nonlinear chemistry and pollution control countermeasure in China. Atmos. Environ. 99, 466–473. https://doi.org/10.1016/j.atmosenv.2014.10.013.
Xie, M., Shu, L., Wang, T.J., Liu, Q., Gao, D., Li, S., Zhuang, B.L., Han, Y., Li, M.M., Chen, P.L., 2017. Natural emissions under future climate condition and their effects on surface ozone in the Yangtze River Delta region, China, Atmos. Environ. Times 150, 162–180. https://doi.org/10.1016/j.atmosenv.2016.11.053.
Xie, Y., Dai, H., Zhang, Y., Wu, Y., Hanaoka, T., Masui, T., 2019. Comparison of health and economic impacts of PM2.5 and ozone pollution in China. Environ. Int. 130 https://doi.org/10.1016/j.envint.2019.05.075.
Xing, J., Wang, S.X., Jang, C., Zhu, Y., Hao, J.M., 2011a. Nonlinear response of ozone to precursor emission changes in China: a modeling study using response surface methodology. Atmos. Chem. Phys. 11, 5027–5044. https://doi.org/10.5194/acp-11-5027-2011.
Xing, J., Zhang, Y., Wang, S.X., Liu, X.H., Cheng, S.H., Zhang, Q.A., Chen, Y.S., Streets, D. G., Jang, C., Hao, J.M., Wang, W.X., 2011b. Modeling study on the air quality impacts from emission reductions and atypical meteorological conditions during the 2008 Beijing Olympics. Atmos. Environ. 45, 1786–1798. https://doi.org/10.1016/j.atmosenv.2011.01.025.
Xing, J., Mathur, R., Pleim, J., Hogrefe, C., Gan, C.M., Wong, D.C., Wei, C., Gilliam, R., Pouliot, G., 2015. Observations and modeling of air quality trends over 1990-2010 across the Northern Hemisphere: China, the United States and Europe. Atmos. Chem. Phys. 15, 2723–2747. https://doi.org/10.5194/acp-15-2723-2015.
Xing, J., Mathur, R., Pleim, J., Hogrefe, C., Wang, J., Gan, C.M., Sarwar, G., Wong, D.C., McKeen, S., 2016. Representing the effects of stratosphere-troposphere exchange on 3-D O3 distributions in chemistry transport models using a potential vorticity-based parameterization. Atmos. Chem. Phys. 16, 10865–10877. https://doi.org/10.5194/acp-16-10865-2016.
Xing, J., Wang, J., Mathur, R., Wang, S., Sarwar, G., Pleim, J., Hogrefe, C., Zhang, Y., Jiang, J., Wong, D.C., Hao, J., 2017. Impacts of aerosol direct effects on tropospheric ozone through changes in atmospheric dynamics and photolysis rates. Atmos. Chem. Phys. 17, 9869–9883. https://doi.org/10.5194/acp-17-9869-2017.
Xu, J., Tie, X., Gao, W., Lin, Y., Fu, Q., 2019. Measurement and model analyses of the ozone variation during 2006 to 2015 and its response to emission change in megacity Shanghai, China. Atmos. Chem. Phys. 19, 9017–9035. https://doi.org/10.5194/acp-19-9017-2019.
Xu, Z., Huang, X., Nie, W., Shen, Y., Zheng, L., Xie, Y., Wang, T., Ding, K., Liu, L., Zhou, D., Qi, X., Ding, A., 2018. Impact of biomass burning and vertical mixing of residual-layer aged plumes on ozone in the Yangtze River delta, China: a tethered-balloon measurement and modeling study of a multiday ozone episode. J. Geophys. Res. Atmos. 123, 11786–11803. https://doi.org/10.1029/2018jd028994.
Yang, W., Chen, H., Wang, W., Wu, J., Li, J., Wang, Z., Zheng, J., Chen, D., 2019. Modeling study of ozone source apportionment over the Pearl River Delta in 2015. Environ. Pollut. 253, 393–402. https://doi.org/10.1016/j.envpol.2019.06.091.
Yang, X., Wu, K., Wang, H., Liu, Y., Gu, S., Lu, Y., Zhang, X., Hu, Y., Ou, Y., Wang, S., Wang, Z., 2020. Summertime ozone pollution in Sichuan Basin, China: meteorological conditions, sources and process analysis. Atmos. Environ. 226 https://doi.org/10.1016/j.atmosenv.2020.117392.
Yang, Y., Liao, H., Li, J., 2014. Impacts of the East Asian summer monsoon on interannual variations of summertime surface-layer ozone concentrations over China. Atmos. Chem. Phys. 14, 6867–6879. https://doi.org/10.5194/acp-14-6867-2014.
Yu, K., Jacob, D.J., Fisher, J.A., Kim, P.S., Marais, E.A., Miller, C.C., Travis, K.R., Zhu, L., Yantosca, R.M., Sulprizio, M.P., Cohen, R.C., Dibb, J.E., Fried, A., Mikoviny, T., Ryerson, T.B., Wennberg, P.O., Wisthaler, A., 2016. Sensitivity to grid resolution in the ability of a chemical transport model to simulate observed oxidant chemistry under high-isoprene conditions. Atmos. Chem. Phys. 16, 4369–4378. https://doi.org/10.5194/acp-16-4369-2016.
Yu, M., Zhu, Y., Lin, C.-J., Wang, S., Xing, J., Jang, C., Huang, J., Huang, J., Jin, J., Yu, L., 2019. Effects of air pollution control measures on air quality improvement in Guangzhou, China. J. Environ. Manag. 244, 127–137. https://doi.org/10.1016/j.jenvman.2019.05.046.
Zender, C.S., Bian, H., Newman, D., 2003. Mineral dust entrainment and deposition (DEAD) model: description and 1990s dust climatology. J. Geophys. Res. Atmos. 108 https://doi.org/10.1029/2002JD002775.
Zeng, P., Lyu, X.P., Guo, H., Cheng, H.R., Jiang, F., Pan, W.Z., Wang, Z.W., Liang, S.W., Hu, Y.Q., 2018. Causes of ozone pollution in summer in Wuhan, Central China. Environ. Pollut. 241, 852–861. https://doi.org/10.1016/j.envpol.2018.05.042.
Zeren, Y., Guo, H., Lyu, X., Jiang, F., Wang, Y., Liu, X., Zeng, L., Li, M., Li, L., 2019. An ozone "pool" in south China: investigations on atmospheric dynamics and photochemical processes over the Pearl River estuary. J. Geophys. Res. Atmos. 124, 12340–12355. https://doi.org/10.1029/2019jd030833.
Zhang, B., Wang, Y., Hao, J., 2015a. Simulating aerosol-radiation-cloud feedbacks on meteorology and air quality over eastern China under severe haze conditionsin winter. Atmos. Chem. Phys. 15, 2387–2404. https://doi.org/10.5194/acp-15-2387-2015.
Zhang, H., Linford, J.C., Sandu, A., Sander, R., 2011. Chemical mechanism solvers in air quality models. Atmosphere 2, 510–532. https://doi.org/10.3390/atmos2030510.

Zhang, J., Choi, M.S., Ji, Y.M., Zhang, R.Y., Zhang, R.Q., Ying, Q., 2021a. Assessing the uncertainties in ozone and SOA predictions due to different branching ratios of the cresol pathway in the toluene-OH oxidation mechanism. ACS Earth Space Chem 5, 1958–1970. https://doi.org/10.1021/acsearthspacechem.1c00092.

Zhang, L., Liu, L.C., Zhao, Y.H., Gong, S.L., Zhang, X.Y., Henze, D.K., Capps, S.L., Fu, T. M., Zhang, Q., Wang, Y.X., 2015b. Source attribution of particulate matter pollution over North China with the adjoint method. Environ. Res. Lett. 10, 8. https://doi.org/10.1088/1748-9326/10/8/084011.

Zhang, L., Li, Q., Wang, T., Ahmadov, R., Zhang, Q., Li, M., Lv, M., 2017. Combined impacts of nitrous acid and nitryl chloride on lower-tropospheric ozone: new module development in WRF-Chem and application to China. Atmos. Chem. Phys. 17, 9733–9750. https://doi.org/10.5194/acp-17-9733-2017.

Zhang, L., Zhao, T., Gong, S., Kong, S., Tang, L., Liu, D., Wang, Y., Jin, L., Shan, Y., Tan, C., Zhang, Y., Guo, X., 2018. Updated emission inventories of power plants in simulating air quality during haze periods over East China. Atmos. Chem. Phys. 18, 2065–2079. https://doi.org/10.5194/acp-18-2065-2018.

Zhang, Q., Zheng, Y., Tong, D., Shao, M., Wang, S., Zhang, Y., Xu, X., Wang, J., He, H., Liu, W., Ding, Y., Lei, Y., Li, J., Wang, Z., Zhang, X., Wang, Y., Cheng, J., Liu, Y., Shi, Q., Yan, L., Geng, G., Hong, C., Li, M., Liu, F., Zheng, B., Cao, J., Ding, A., Gao, J., Fu, Q., Huo, J., Liu, B., Liu, Z., Yang, F., He, K., Hao, J., 2019. Drivers of improved PM2.5 air quality in China from 2013 to 2017. Proc. Natl. Acad. Sci. U. S. A 116, 24463. https://doi.org/10.1073/pnas.1907956116.

Zhang, X., Fung, J.C.H., Lau, A.K.H., Hossain, M.S., Louie, P.K.K., Huang, W., 2020. Air quality and synergistic health effects of ozone and nitrogen oxides in response to China's integrated air quality control policies during 2015-2019. Chemosphere 268. https://doi.org/10.1016/j.chemosphere.2020.129385, 129385-129385.

Zhang, Y., Chen, Y., Sarwar, G., Schere, K., 2012. Impact of gas-phase mechanisms on weather research forecasting model with chemistry (WRF/chem) predictions: mechanism implementation and comparative evaluation. J. Geophys. Res. Atmos. 117 https://doi.org/10.1029/2011JD015775.

Zhang, Y., Zhang, X., Wang, K., Zhang, Q., Duan, F.K., He, K.B., 2016. Application of WRF/Chem over East Asia: Part II. Model improvement and sensitivity simulations. Atmos. Environ. 124, 301–320. https://doi.org/10.1016/j.atmosenv.2015.07.023.

Zhang, Y.Q., Shindell, D., Seltzer, K., Shen, L., Lamarque, J.F., Zhang, Q., Zheng, B., Xing, J., Jiang, Z., Zhang, L., 2021b. Impacts of emission changes in China from 2010 to 2017 on domestic and intercontinental air quality and health effect. Atmos. Chem. Phys. 21, 16051–16065. https://doi.org/10.5194/acp-21-16051-2021.

Zhao, Y., Zhang, L., Zhou, M., Chen, D., Lu, X., Tao, W., Liu, J., Tian, H., Ma, Y., Fu, T.M., 2019. Influences of planetary boundary layer mixing parameterization on summertime surface ozone concentration and dry deposition over North China. Atmos. Environ. 218 https://doi.org/10.1016/j.atmosenv.2019.116950.

Zheng, B., Zhang, Q., Tong, D., Chen, C., Hong, C., Li, M., Geng, G., Lei, Y., Huo, H., He, K., 2017. Resolution dependence of uncertainties in gridded emission inventories: a case study in Hebei, China, Atmos. Chem. Phys. 17, 921–933. https://doi.org/10.5194/acp-17-921-2017.

Zheng, B., Cheng, J., Geng, G., Wang, X., Li, M., Shi, Q., Qi, J., Lei, Y., Zhang, Q., He, K., 2021. Mapping anthropogenic emissions in China at 1 km spatial resolution and its application in air quality modeling. Sci. Bull. 66, 612–620. https://doi.org/10.1016/j.scib.2020.12.008.

Zhong, M., Saikawa, E., Liu, Y., Naik, V., Horowitz, L.W., Takigawa, M., Zhao, Y., Lin, N. H., Stone, E.A., 2016. Air quality modeling with WRF-Chem v3.5 in East Asia: sensitivity to emissions and evaluation of simulated air quality. Geosci. Model Dev. (GMD) 9, 1201–1218. https://doi.org/10.5194/gmd-9-1201-2016.

Zhu, B., Gao, J., Hou, X., Kang, H., Pan, C., 2017. Source apportionment of tropospheric ozone by chemical transport model: from global to city cluster. In: Bouarar, I., Wang, X., Brasseur, G.P. (Eds.), Air Pollution in Eastern Asia: an Integrated Perspective. Springer International Publishing, Cham, pp. 191–217. https://doi.org/10.1007/978-3-319-59489-7_9.

Zhu, J., Liao, H., 2016. Future ozone air quality and radiative forcing over China owing to future changes in emissions under the Representative Concentration Pathways (RCPs). Journal of J. Geophys. Res. Atmos. 121, 1978–2001. https://doi.org/10.1002/2015jd023926.

Zhu, J., Chen, L., Liao, H., Dang, R., 2019. Correlations between PM2.5 and ozone over China and associated underlying reasons. Atmosphere 10, 352, 10.10.3390/atmos10070352.